Norwegian University of Life Sciences

Master's Thesis 2023 30 ECTS
Faculty of Chemistry, Biotechnology and Food Science

The effects of Rapamycin on Lifespan and Healthspan in *Caenorhabditis elegans atg-18* mutants

Erica Caci Back
Chemistry and Biotechnology

The effects of Rapamycin on Lifespan and Healthspan in *Caenorhabditis elegans atg-18* mutants

Erica Caci Back

Acknowledgments

The study presented in this thesis was performed in the Evandro Fang Lab at the Faculty of Medicine at the University of Oslo, Akershus University Hospital with Professor Evandro Fei Fang and PhD-student Tomás Alejandro Schmauck-Medina as my supervisors.

First, I would like to thank my main supervisor and group leader Evandro Fei Fang for kindly inviting me to be a part of your group and for always being supportive and helpful. I admire your hard work, knowledge and all your achievements.

Secondly, I want to thank my daily supervisor Tomás Alejandro Schmauck-Medina for guiding me through this thesis. Not only have you taught me everything I know within this field, but you have also always taken your time to answer my questions and guide me when I'm stuck. Thank you for your support, positivity, advice, and daily laughs.

Sofie Hindkjær Lautrup, thank you for all the hours you have spent teaching me how to work in the cell lab and for guiding me through this part of the thesis. I am beyond grateful for your helpfulness, knowledge, and kindness, and for making this contribution to the thesis possible.

All other members of the Evandro Fang Lab, you deserve a BIG thank you. You have all been nothing but kind and helpful from day one, and all of you have contributed to making every day in the lab a good one. You are all hard-working people who I wish nothing but the best.

I would also like to thank my NMBU-supervisor Åsmund Røhr Kjendseth for showing interest in this study, guiding me in the writing-process and helping me with my questions.

Finally, I want to thank my family for all the help and support you have shown through my years as a student, my friends for all the great moments we have shared, and my boyfriend Kristian for being the best motivator through all these years.

Thank you all!

Erica Caci Back

Ås, May 2023

Abstract

Aging is a biological process causing loss of physical integrity, reduced function, and higher vulnerability to death. Aging also increases the risk of major human diseases including cancer, diabetes, cardiovascular disorders, and neurodegenerative disorders like dementia. Research on aging and age-related diseases is important to improve human health during aging to minimize the global socioeconomic burden and challenges in healthcare. Autophagy is a cellular clearance pathway which promotes homeostasis in the cells and is proposed as a hallmark of aging. A disruption of autophagy is shown to accelerate age-related aggregation of proteins and shorten lifespan in several model organisms. An increase in autophagy e.g., by the autophagy-inducer rapamycin has shown suppressed protein aggregation as well as promoted health and longevity. Studies have shown that induction of autophagy by treatment with rapamycin in the widely used nematode *Caenorhabditis elegans* extends lifespan and healthspan parameters.

This study aimed to investigate the effects of rapamycin treatment with a malfunctioning autophagy-machinery to see whether the treatment can affect lifespan and/or healthspan without affecting autophagy. *C. elegans atg-18(gk378)* with a loss-of-function mutation causing a malfunctional autophagy-machinery were investigated. Lifespan assay, as well as the healthspan assays pharyngeal pumping and thrashing were performed in the mutant and in a WT strain to examine the effects of the treatment. The lifespan assay showed a decreased lifespan for the mutants treated with rapamycin, suggesting that rapamycin might affect other mechanisms related to the process of aging with a negative effect. Considering that the thrashing assay might be a more reliable healthspan parameter than the pumping assay, rapamycin-treatment seemed to increase healthspan of the mutants as well as for the WT.

To validate the effect of rapamycin on autophagy and the mammalian ATG-18 homolog WIPI2, HeLa cells with GFP-tagged WIPI2B were treated with rapamycin. Imaging of the cells clearly showed an increase in autophagy after 24 hours of treatment. Imaging as well as Western Blots suggested that 2 hours of treatment is not sufficient to show an effect of rapamycin-treatment.

This study suggests that rapamycin decreases the lifespan of *C. elegans atg-18(gk378)* mutants, but to some degree promote healthier aging. The mechanisms seemingly affected by rapamycin in the *C. elegans* mutants may be interesting for further investigation. Not only in *C. elegans*, but also using other model organisms to investigate the replicability of the results in other models.

Sammendrag

Aldring er en biologisk prosess som forårsaker redusert funksjonsnivå, lavere levedyktighet og høyere dødelighet. Aldring øker også risikoen for alvorlige sykdommer hos mennesker som kreft, diabetes, hjerte- og karsykdommer og nevrodegenerative sykdommer som demens. Forskning på aldring og aldringsrelaterte sykdommer er viktig for å forbedre menneskers helse under aldring, og for å minimere den globale sosioøkonomiske byrden og utfordringene som oppstår i helsevesenet. Autofagi er en cellulær «resirkuleringsprosess» som opprettholder homeostase i cellene, og ses på som et kjennetegn på aldring. Hindring av autofagi-prosessen har vist seg å øke aldersrelatert aggregering av proteiner i cellene og forkorter levetiden til flere modellorganismer. En økning i autofagi ved hjelp av for eksempel autofagi-induseren rapamycin, har vist seg å dempe proteinaggregeringen samt fremme god helse og lengre levetid. Studier har vist at induksjon av autofagi ved behandling med rapamycin i den mye brukte nematoden *Caenorhabditis elegans* forlenger dens levetid og forbedrer dens helsetilstand.

Målet med denne studien var å undersøke effekten av rapamycinbehandling når autofagimaskineriet ikke er fungerende for å se om behandlingen fortsatt kan påvirke levetid og/eller helse uten muligheten til å påvirke autofagi. *C. elegans atg-18(gk378)* med en tap-av-funksjon-mutasjon som forårsaker et ikke-funksjonelt autofagimaskineri ble brukt i studien. Analyse av levetid og de ulike analysene for helsetilstand «pumping» og «thrashing» (også kalt svømming) ble utført med mutanten samt en villtype for å undersøke effektene av behandlingen. Resultatene av levetidsanalysene viste en redusert levetid for mutantene behandlet med rapamycin, noe som tyder på at rapamycin kan påvirke andre mekanismer relatert til aldringsprosessen, med en negativ effekt. Tatt i betraktning at «thrashing»-analysen kan være en mer pålitelig analyse for helsetilstand enn «pumping»-analysen, så det ut til at rapamycinbehandling økte helsetilstanden til både mutantene og villtypen.

For å validere effekten av rapamycin på autofagi og på WIPI2, det menneskelige homologe proteinet av ATG-18, ble HeLa-celler med GFP-merket WIPI2B behandlet med rapamycin. Mikroskopi-bilder av cellene viste en tydelig økning i autofagi etter 24 timers behandling. Bilder og Western Blots viste at en 2-timers behandling ikke var tilstrekkelig for å vise en effekt av rapamycin-behandlingen.

Resultatene fra denne studien antyder at rapamycin reduserer levetiden til *C. elegans atg-18(gk378)* mutanter, men til en viss grad også fremmer en sunnere aldring. Mekanismene som tilsynelatende påvirkes av rapamycin i *C. elegans* mutantene kan være interessante for videre

forskning. Ikke bare i *C. elegans*, men også i andre modellorganismer for å undersøke om resultene er reproduserbare også i andre modeller.

Abbreviations

µL	Microliter
µM	Micromolar
AD	Alzheimer's disease
ALS	Amyotrophic lateral sclerosis
AMBRA1	Autophagy and Beclin 1 Regulator 1
AMPK	AMP-activated kinase
ATG	Autophagy related
BCA	Bicinchoninic acid
BCL-2	B-cell lymphoma 2
BECN1	Beclin 1
bp	Base pairs
$CaCl_2$	Calcium chloride
C. elegans	Caenorhabditis elegans
CRISPR	Clustered regularly interspaced short palindromic repeats
dH_2O	Distilled water
ddH_2O	Double distilled water
DDT	Dichlorodiphentyltrichloroethane
DEPTOR	DEP domain-containing mTOR-interacting protein
dTOR	*Drosophila* target of rapamycin
DMEM	Dulbecco's Modified Eagle Medium
DMSO	Dimethyl sulfoxide
EBSS	Earle's balanced salt solution
EDTA	Ethylenediaminetetraacetic acid
ELISA	Enzyme Linked Immunosorbent Assay
ER	Endoplasmic reticulum
EtOH	Ethanol
FBS	Fetal bovine serum
FKBP12	FK506 binding protein (12 kDa)

FUDR	Floxuridine
g	gravitational force
GFP	Green fluorescent protein
HeLa	Henrietta Lacks
HOPS	Homotypic fusion and protein sorting
KH_2PO_4	Dipotassium phosphate
kDa	Kilodalton
KH_2PO_4	Potassium dihydrogen phosphate
L	Liter
LB	Lysogeny broth
LIRs	LC3-interacting motifs
LC3	Microtubule-associated protein 1A/1B-light chain 3
LKB1	Liver kinase B1
LST8	Lethal with SEC13 protein 8
M	Molar
MeOH	Methanol
mg	Milligram
$MgSO_4$	Magnesium sulfate
mL	Milliliter
MLST8	MTOR associated protein, LST8 homolog
ms	Milli seconds
mTOR	Mechanistic target of rapamycin
mTORC1	Mechanistic target of rapamycin complex 1
mTORC2	Mechanistic target of rapamycin complex 2
Na_2HPO_4	Disodium hydrogen phosphate
NaCl	Sodium chloride
NaOH	Sodium hydroxide
NFW	Nuclease free water
NGM	Nematode Growth Medium
nm	Nano meters
P/S	Penicillin and Streptomycin

PBS	Phosphate-buffered saline
PD	Parkinson's disease
PE	Phosphatidylethanolamine
PI3P/PtdIns3P	Phosphatidylinositol 3-phosphate
PIK3C3	Phosphatidylinositol 3-kinase
PRAS40	Proline-rich Akt substrate of 40 kDa
PVDF	Polyvinylidene difluoride
RAB	Ras-associated binding
Rapa	Rapamycin
RIPA	Radioimmunoprecipitation assay
rpm	revolutions per minute
RAPTOR	Regulatory-associated protein of mTOR
SDS-PAGE	Sodium dodecyl-sulfate polyacrylamide gel electrophoresis
SNARE	Soluble N-ethylmaleimide-sensitive-factor attachment protein receptor
SQSTM1	Sequestome 1
TBS	Tris Buffered Saline
TBST	Tris Buffered Saline Tween 20
TSC2	Tuberous Sclerosis Complex 2/Tuberin
ULK1	Unc-51-like kinase 1
V	Volts
Veh	Vehicle
WD	Tryptophan-Aspartic acid
WIPI	WD-repeat protein Interacting with Phosphoinositides
WT	Wildtype

Table of contents

1 Introduction

1.1 Aging

Aging is a biological process characterized by progressive loss of physical integrity resulting in reduced function and quality of life, as well as heightened vulnerability to death. Aging was formerly believed to be a consequence of inevitable accumulation of mutations and other damage. Now, the process and rate of aging is also known to be controlled by evolutionary conserved biochemical processes and genetic pathways and affects most living organisms at different rates (Lopez-Otin et al., 2013; Niccoli & Partridge, 2012). Molecular and cellular processes and biomarkers linked to the process of aging are found in different model organisms and mammals showing that even though aging still is considered an inevitable process, different mechanisms and treatment can maintain homeostasis in cells and tissue and thus promote healthy aging (Hou et al., 2019). In late age, the force of natural selection declines. The process of aging can develop because of this, and as a consequence of the accumulation of mutations during later aging that leads to lower fitness. There are also mutations increasing fitness at a young age at the expense of aging at a subsequently higher rate (Niccoli & Partridge, 2012).

In 2013, Lopez-Otin et al. summarized nine tentative cellular and molecular hallmarks thought to contribute to the process of aging. These hallmarks include genomic instability, telomere attrition, epigenetic alterations, loss of proteostasis, deregulated nutrient sensing, mitochondrial dysfunction, cellular senescence, stem cell exhaustion, and altered intercellular communication (Lopez-Otin et al., 2013). Recently, three new hallmarks of aging have been proposed in addition to the first nine: disabled macroautophagy, chronic inflammation and dysbiosis (Lopez-Otin et al., 2023). In addition to these 12 hallmarks proposed by Lopez-Otin et al., Schmauck-Medina et al., summarizes three additional hallmarks: Dysregulation of RNA processing, microbiome disturbances and altered mechanical properties (Schmauck-Medina et al., 2022). Combined, these hallmarks serve as common features of aging across different organisms (Lopez-Otin et al., 2023). While it presumes that aging is irreversible, there is evidence that DNA methylation (DNAm)-based biological age is likely reversible, at least in a short period after the vanishing of trauma such as surgery, pregnancy, and COVID-19 (Poganik et al., 2023).

1.1.1 Aging as a risk factor for disease

A major concern when it comes to aging is that it significantly increases the risk of several major human diseases including cancer, diabetes, cardiovascular disorders, and neurodegenerative disorders including different types of dementia. The widely considered thought that aging is caused by accumulating cellular damage over time links the aging process to the process of cancer, where some cells take advantage of cellular damage and may lead to development of the disease (Lopez-Otin et al., 2013).

Loss of proteostasis and compromised autophagy are two of the proposed hallmarks of aging. These hallmarks are of interest as they are closely linked to the causes of neurodegenerative diseases and brain aging. Proteostasis include maintenance of correct protein folding, assembly, degradation in the cell and trafficking. Under lack of maintenance of proteostasis, misfolded, mislocalized and aggregated proteins will be present in the cells. Studies have shown a loss of proteostasis during aging in several tissues. Diseases like Alzheimer's disease (AD), Parkinson's disease (PD), Huntington's disease, and amyotrophic lateral sclerosis (ALS) are strongly connected to age-dependent protein aggregation. Autophagy has several features, including degradation of misfolded proteins, organelles, DNA, and removal of bulk protein aggregates, and thereby contribute to maintenance of proteostasis, but also homeostasis. Genetic disruption of autophagy is shown to accelerate age-related aggregation of proteins, as well as shorten lifespan in model organisms like worms, flies, and mice. An increase in autophagy has the opposite effect and shows suppressed protein aggregation as well as promoted health and longevity (Aman et al., 2021). Compromised autophagy is one of the more recent proposed hallmarks originally considered under the loss of proteostasis hallmark. Since autophagy not only contributes to increased proteostasis, but also regulates other hallmarks of aging, like deregulated nutrient sensing as well as DNA repair, it is proposed as an independent hallmark (Schmauck-Medina et al., 2022). Detailed mechanisms of autophagy will be described in a later section.

1.1.2 Research on aging

Approximately 40 years ago, a new era in aging research began. The isolation of the first long-lived strains in the roundworm *Caenorhabditis elegans* (*C. elegans*) started this era (Klass, 1983). In aging research, in addition to *C. elegans,* mice (commonly *Mus musculus*), and fruit flies (*Drosophila melanogaster*) are widely used as models. These models have in common that

they are comparatively easy to work with, have relatively short lifespan, and precisely described transcriptomic and genomic sequencing data of high quality. The mechanisms of aging can be investigated in such models using among others CRISPR/Cas-systems and other genetic engineering tools. There is also a commercial availability of knock-in and knock-out models. The use of the mentioned model organisms has a lot of advantages in aging research, but there is also a question about to which extent this research is representative for higher animals, and humans with a 40,000-fold variation in aging rates. Research that shows an increase in lifespan for short-lived species do not necessarily show the same effects in long-lived organisms (Holtze et al., 2021).

Research on aging often uses lifespan as a measure, as it is a precise and universal parameter that reflects an animal's health (Keith et al., 2014). The focus on lifespan as the sole parameter in aging research is questioned as changes in lifespan, especially lifespan extension, does not always correlate with changes in the quality of life (healthspan) in the same direction. E.g., it is shown that all tested long-lived *C. elegans* mutants increased the proportion of time spent in a frail state, which reveal the importance of including healthspan parameters in aging research as well as the lifespan; an increased lifespan could lead to a negative consequence for the society if it only results in a longer frail state (Bansal et al., 2015). Healthspan is the other central aspect of aging, despite its unclear definition ranging from 'the period of midlife vigor that precedes significant functional decline' (Iwasa et al., 2010), to 'the length of time an individual is able to maintain good health' (Tatar, 2009). More recent studies on aging have started to focus more on the measure of healthspan over lifespan, indicating that healthspan is of a great importance in aging. When it comes to clinical, social, and fiscal perspectives of human health, healthspan is the most prominent focus in the aging research considering the rapidly aging of the global population (Keith et al., 2014).

Although some of the mechanisms behind aging have become known, aging is an extremely complex process, and many cellular functions remain unclear. Further studies on this field may not only contribute to answer questions regarding the pathways leading to functional declines but are also crucial to reveal the relationship between aging and disease (Glenn et al., 2004). Over the last decades, one of the most remarkable human accomplishments is that average human lifespan has increased. This is not only a success, as it leads to an increasing number of patients with age-related diseases which contributes to a burden on the society (Schmauck-Medina et al., 2022). Deeper knowledge about the relationship between aging and disease is important for identifying pharmaceutical targets to develop treatment for age-related diseases,

but also to improve human health during aging to minimize the global socioeconomic burden and challenges in healthcare (Aman et al., 2021; Lopez-Otin et al., 2013).

1.2 *Caenorhabditis elegans*

Caenorhabditis elegans (*C. elegans*) is a small free-living, transparent nematode round worm (Brenner, 1974) widely used as a model organism in research (Kaletta & Hengartner, 2006). *C. elegans* was first thought to be a soil nematode, but more recent research shows that it principally is a colonizer of decaying plant matter and other microbe-rich habitats (Félix & Braendle, 2010). Sydney Brenner first introduced the nematode in 1963 as a model for studying development and neurobiology (Kaletta & Hengartner, 2006), and in 1974 he published methods for isolation, complementation and mapping of *C. elegans* mutants (Brenner, 1974).

The adult worm has a size of only 1 mm and is usually observed with a microscope (Corsi et al., 2015). It is a sophisticated multicellular animal containing 959 somatic cells and about 2000 germ cells in the hermaphrodite, and 1031 somatic cells and about 1000 germ cells in the male (Alberts et al., 2002). The somatic cells form muscle, hypodermis, intestine, the reproductive system, glands and many other organs and tissues (Kaletta & Hengartner, 2006). Many of these somatic cells forms the most complex tissue of *C. elegans*; the nervous system containing 320 neurons and 56 glia-like cells (hermaphrodite) (Naranjo-Galindo et al., 2022). **Figure 1** shows the basic anatomy of a *C. elegans* hermaphrodite.

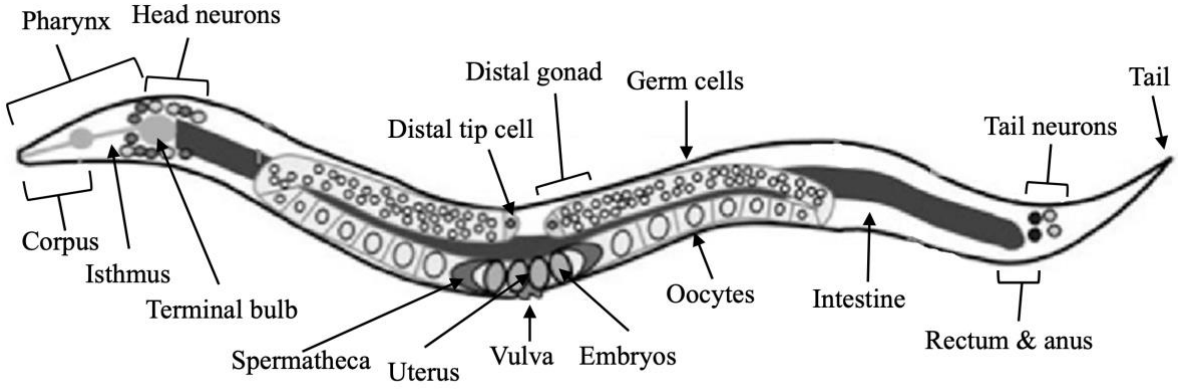

***Figure 1*. C. elegans hermaphrodite anatomy.** *The figure shows the basic anatomy of a C. elegans hermaphrodite. The figure is modified from (Yen et al., 2011).*

The lifespan of *C. elegans* is relatively short, approximately 18-20 days when grown at 20°C (Zhang et al., 2020). The life-history of a *C. elegans* worm starts with a fertilized egg, which consists of one single cell. Through repeated cell divisions, the egg gives rise to 558 cells which inside the eggshell forms a small worm (Alberts et al., 2002). After hatching, the worm develops through four larval stages: L1, L2, L3 and L4, separated by molts. After L4, the worm becomes a reproductive adult. At 20°C, the development from fertilized egg to reproductive adult takes approximately three days. In case of a non-favorable environment like lack of food or stress due to overpopulation, the L1 larvae can go into the dauer stage (Baugh, 2013). The dauer stage is an alternative development stage where the worm become stress resistant. In this stage, it can survive for several months before going back to normal developmental cycle when the environment is back to favorable conditions (Baugh, 2013; Riddle et al., 1981). The *C. elegans* life cycle is shown in **Figure 2**.

C. elegans can be grown at different temperatures, but the growth rate and fertility are dependent on the temperature. They can usually be grown at temperatures between 12°C and 25°C, and an increase of 10°C speeds up growth twofold. This temperature dependency makes the rate of animal development possible to control. A continual growth in temperatures above 25°C makes the worms sterile (Corsi et al., 2015), while development halts below 8°C (Félix & Braendle, 2010).

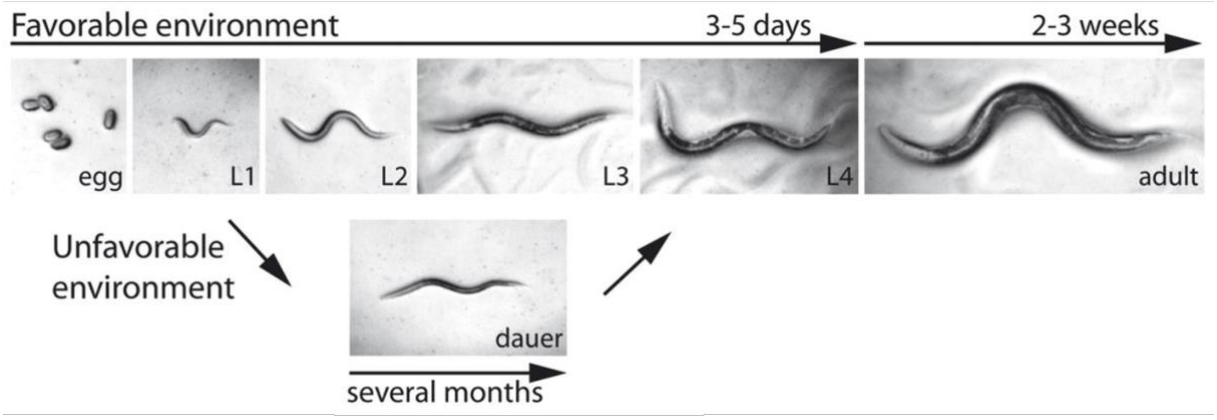

Figure 2. Life cycle of C. elegans. *The life cycle of C. elegans starts as a fertilized egg which through repeated cell divisions give rise to a small worm inside the eggshell. After hatching, the worm develops through the four larval stages: L1, L2, L3 and L4. After L4, the worm becomes a reproductive adult. In case of an unfavorable environment, the L1 larvae can go into dauer stage (Baugh, 2013; Riddle et al., 1981). The figure is modified from (Fielenbach & Antebi, 2008).*

1.2.1 *C. elegans* as a model organism

Several features of the *C. elegans* nematode make it an excellent model organism in research. The worm is relatively simple and precisely structured (Alberts et al., 2002) and is currently used in a huge variety of research compared to when it was first introduced as a model. Biological processes such as apoptosis, cell cycle, cell signaling, cell polarity, gene regulation, metabolism, sex determination, aging and age-related diseases are some fields were *C. elegans* is used as a model organism. Both when it comes to basic biology and medical areas, many key discoveries were first made in this nematode, as exemplified by at least 3 Nobel prize awards that were directly related to studies in *C. elegans* (Kaletta & Hengartner, 2006).

In 1998, the entire genome sequence of *C. elegans* was completely sequenced, and the around 20,000 genes of the worm became known. Not only did this lead to the worm being an ideal model for genetic studies, but out of all these genes, 60-80% were shown to be evolutionary conserved between *C. elegans* and humans. This is one of the most important characteristics making the worm a useful model organism for studying human disease, drug development and other biological processes in humans (Consortium, 1998). *C. elegans* has no brain-like organ, but it indeed has a sophisticated and functionally evolutionary conserved neuronal ring in the head region, making it a good model for studies within neuroscience. Some of the most classical neurotransmitters are present in *C. elegans*, and the interactions of neurons, synapses and neurotransmitters in the worm are similar to those of mammals (Naranjo-Galindo et al., 2022), making a rationale on the use of *C. elegans* for studies of memory-like behaviors and drug screening (Cao et al., 2023).

C. elegans is relatively simple and tractable. It is easy to culture in the laboratory on a diet of *Escherichia coli* (Kaletta & Hengartner, 2006). Easy culturing together with the rapid reproduction and short lifespan makes *C. elegans* suitable for lifespan assays in aging research, among others. The small size of the worm means that it can be grown in a small place. Most assays using *C. elegans* can easily take place in small agar plates, or in liquid in small wells or tubes (Kaletta & Hengartner, 2006). The transparency of *C. elegans* makes it easy to visualize individual cells and subcellular details. Fluorescent proteins can be used to tag proteins or subcellular compartments for enhanced details (Corsi et al., 2015). The transparency is also contributing to make certain healthspan assays, such as pharyngeal pumping (**1.2.2**) easy to perform.

C. elegans are either hermaphrodites or males, making them sexually dimorphic. The majority of the population are hermaphrodites, while only 0.1% are males (Brenner, 1974). The hermaphrodites produces both eggs and sperm, and can thereby reproduce either by self-fertilization, or by cross-fertilization by mating with a male. The capability of self-fertilization makes *C. elegans* an exceptionally convenient organism for genetic studies since it allows the production of homozygous progeny by a single heterozygous worm (Alberts et al., 2002).

There are no major ethical concerns by doing experiments using *C. elegans* (Zhang et al., 2020), and a certificate for working with laboratory animals is not needed in Norway. *C. elegans* is also the most amenable to cost-effective medium/high-throughput technologies, as well as the fastest, compared to other animal models (Kaletta & Hengartner, 2006). The diversity of advantages described in this section has led to several breakthrough discoveries in the aging-field among others, using *C. elegans,* and are arguments for why *C. elegans* is such an excellent organism for aging research (Zhang et al., 2020).

1.2.2 Healthspan assays in aging research using *C. elegans*

C. elegans is as mentioned a widely used model organism in aging research. The use of the nematode has given generous information about genes that determine lifespan, but less when it comes to how aging in the worm affects the cellular functions. One established fact is that with increasing age, there is a gradually decrease of body movement in *C. elegans.* The rate of age-related decline in body movement is shown to be a good predictor for lifespan, which proposes that there may be shared components between decline in body movement and senescence in the organism (Glenn et al., 2004).

There are a wide range of approaches when it comes to examining the health of *C. elegans.* Two of the approaches which are used in this study are pharyngeal pumping and thrashing (also known as swimming) assays. Pharyngeal pumping is how feeding occurs in *C. elegans* and is also a known and well-used indicator of healthspan and aging in the nematode (Chow et al., 2006). A positive correlation between pharyngeal pumping and lifespan in *C. elegans* is shown, implying that the pharyngeal pumping rate decline with aging. It is reported that from adult day 2 until day 7, the pharyngeal pumping rate declined gradually, while from day 7 until day 10, the rate declined rapidly. In the days after day 10, the pumping rate ceased completely (Huang et al., 2004). The feeding in *C. elegans* occurs via the neuromuscular pump, pharynx, which consists of the corpus, the isthmus, and the terminal bulb. A contraction of the muscles of the

corpus, anterior isthmus, and terminal bulb at a near simultaneous rate defines the beginning of a pump. The muscles of the pharynx are radially oriented, meaning contractions of the corpus and isthmus pulls the lumen open to a triangular cross-section, allowing liquid and suspended bacteria from the outside to be sucked in. The rate of the pumping determines the amount of food intake and the growth rate (Avery & You, 2005-2018).

Another method used to determine healthspan in *C. elegans* is the thrashing assay. This method measures the motility of the worm, as it starts swimming (thrashing) when placed in liquid media. The swimming is the worm's response as it adapts to the new liquid environment. These thrashing-movements are estimated and can be used as an index of the effects of drugs or mutations on the motility (Buckingham & Sattelle, 2009). Thrashing rate is shown to gradually decline with age (Bansal et al., 2015; Hering et al., 2022), and it is shown that long-lived mutants can keep a higher motility rate at older ages than the wildtype (WT) (Ibáñez-Ventoso et al., 2016). The age-dependent decline in thrashing rate is shown to be partially caused by sarcopenic deterioration of muscle (Restif et al., 2014).

1.3 HeLa cells

Originating from the cervical cancer tumor of patient Henrietta Lacks over 70 years ago, HeLa cells were the first human cell line growing well in a lab (Callaway, 2013). Not only was it the first cell line, but also the most used model cell line for studying human cellular and molecular biology (Landry et al., 2013). The development of the polio virus vaccine was one of the first accomplishments using HeLa cells (Scherer et al., 1953). Since then, the cells have distributed worldwide as a laboratory model organism and has provided understanding of many important biological processes and breakthroughs in molecular biology. Some of these breakthroughs include the connection between human papilloma virus and cervical cancer, and chromosome degradation prevention by telomerase (Landry et al., 2013). Thousands of other cell lines have been established, but HeLa is still the widely used cell line (Masters, 2002).

In most somatic cells, the telomeres are shortened for every cell division, ultimately making the cells enter senescence. By expressing the enzyme telomerase, telomere shortening is prevented in HeLa cells, as well as in other cancer cells. This feature prevents the cells from entering senescence, and thus making them immortal (Ivanković et al., 2007).

1.4 Autophagy

Autophagy is a natural, evolutionarily conserved cellular process in all eukaryotic cells (Reggiori & Klionsky, 2002; Takacs et al., 2019). The word "autophagy" comes from the Greek words *auto*, meaning 'self', and *phagein*, meaning 'to eat'. This process is a highly selective cellular clearance pathway which promotes homeostasis in the cell by a lysosome-mediated degradation of molecules and subcellular elements. These molecules and subcellular elements include proteins, nucleic acids, lipids, and organelles, and the degradation of these elements ensures differentiation and development (Aman et al., 2021). Autophagy is also a provider of cellular energy, making the process essential for cell survival during nutrient starvation (Menzies et al., 2015). Based on the cargo sequestration, there are distinguished three types of autophagy: microautophagy, chaperone-mediated autophagy and macroautophagy. Of these three types, macroautophagy is the best studied in the context of aging. The process of macroautophagy involves degradation of cytosolic material via sequestration into double-membrane vesicles (autophagosomes). These autophagosomes then fuse with the lysosomes where the degradation takes place (Hansen et al., 2018). Depending on the cargo, selective autophagy can be further divided into subtypes with different targets. Glycophagy and lipophagy target various macromolecules, mitophagy target mitochondria, ER-phagy target the endoplasmic reticulum, nucleophagy target parts of the nucleus, xenophagy target pathogens, and lysophagy target the lysosomes (Aman et al., 2021).

1.4.1 The process and molecular mechanisms of autophagy

The process of macroautophagy (hereafter termed autophagy) consists of five steps: initiation, membrane nucleation and phagophore formation/elongation, phagophore maturation, fusion with the lysosome and degradation (Hansen et al., 2018; Menzies et al., 2015). As autophagy is a tightly regulated process, there are several signaling pathways involved in the control to avoid both insufficient and excessive levels of autophagy (Yang & Klionsky, 2009). Several autophagy related (ATG) proteins assemble into different complexes which mediates different parts of the process, as illustrated in **Figure 3**. Initiation of the process requires the initiation complex Unc-51-like kinase 1 (ULK1) which is tightly regulated by the two main autophagy-regulators: mechanistic target of rapamycin (mTOR) and AMP-activated kinase (AMPK). Both mTOR and AMPK are conserved nutrient sensors and longevity determinants. AMPK works as an activator of the ULK1 complex, while mTOR acts as an inhibitor (Hansen et al., 2018).

The mechanism of mTOR will be explained in a greater detail in the next section. AMPK phosphorylates and activates ULK1, which in turn causes stimulation of the class III phosphatidylinositol 3-kinase (PIK3C3) complex. The PIK3C3 complex is composed of among others Beclin 1 (BECN1) and Autophagy and Beclin 1 Regulator 1 (AMBRA1), where the functions of BECN1 can be inhibited by B-cell lymphoma 2 (BCL-2). A pool of phosphatidylinositol 3-phosphate (PI3P/PtdIns3P) is produced by the PIK3C3 complex (Aman et al., 2021). This pool recruits WD repeat protein interacting with phosphoinositides (WIPI) proteins (ATG-18 being WIPI1 and WIPI2 in worms). WIPI2B/ATG-18 recruits the ATG12-ATG5-ATG16L1 complex as well as the delivery of lipids in ATG-9-containing vesicles from previous membranes. Microtubule-associated protein 1A/1B-light chain 3 (LC3) is conjugated by WIPI2B's recruitment of the ATG12-ATG5-ATG16L1 complex and then cleaved by the protease ATG4. This causes the formation of LC3-I which later forms LC3-II when conjugated with phosphatidylethanolamine (PE) after recognition by ATG7, ATG3 and the ATG12-ATG5-ATG16L1 complex. At this point, pre-autophagosomal and autophagosomal membranes are formed, ready for incorporation of LC3-II. After incorporation, LC3-II can interact with autophagy receptors like Sequestome 1 (p62/SQSTM-1) which contains LC3-interacting motifs (LIRs) that are bound to cargo targeted for degradation. Ras-associated binding (RAB) and Soluble N-ethylmaleimide-sensitive-factor attachment protein receptor (SNARE) proteins together with a Homotypic fusion and protein sorting (HOPS) complex mediates the fusion of the autophagosomes and lysosomes before lysosomal hydrolases degrades the cargo. The degradation products can then be reused by the cell, and ATG4 cleaves the LC3-II for it to be used in the next lipidation-round (Aman et al., 2021; Grimmel et al., 2015; Hansen et al., 2018).

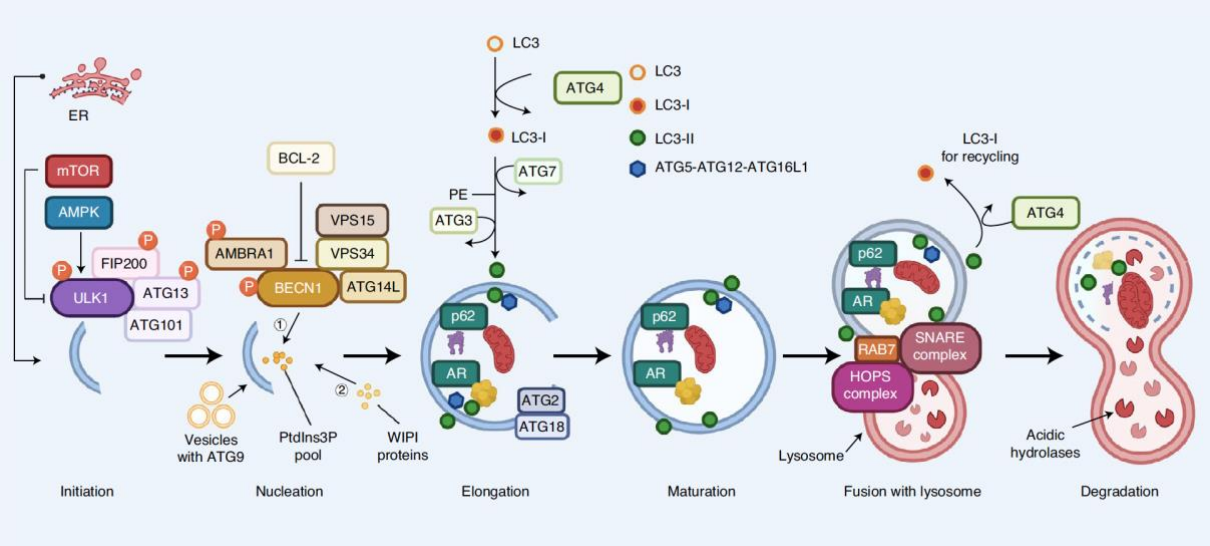

Figure 3. The autophagy machinery. *The initiation of the autophagy requires ULK1, regulated by mTOR and AMPK. AMPK phosphorylates ULK1 which stimulates the PIK3C3 complex consisting of e.g., BECN1 and AMBRA1. PIK3C3 produces a pool of PI3P/PtdIns3P which recruits ATG-18 (WIPI2 in mammals). ATG-18 recruits the ATG12-ATG5-ATG16L1 complex and delivery of lipids in ATG-9 containing vesicles. This complex conjugates LC3, which is then cleaved by ATG4. This leads to formation of LC3-I, which later forms LC3-II when conjugated with PE after recognition by e.g., ATG7 and ATG3. Autophagosomal membranes are formed, ready for incorporation of LC3-II. LC3-II can interact with p62/SQSTM-1 containing LIRs bound to cargo targeted for degradation. RAB, SNARE and HOPS fuse the autophagosomes and lysosomes before lysosomal hydrolases degrades the cargo. ATG4 cleaves LC3-II to be used in the next round. The figure is obtained from (Aman et al., 2021).*

1.4.2 Autophagy regulators

The regulation of autophagy involves several signal transduction pathways (Wang & Zhang, 2019), but as mentioned, there are two main regulators of autophagy induction. While AMPK works as an activator of the process, mTOR is the inhibitor. mTOR is an evolutionarily conserved protein (serine/threonine) kinase (Reggiori & Klionsky, 2002) which is recognized as a master regulator of cell growth and metabolism (Li et. al., 2014). mTOR exists in yeasts (TOR), multicellular animals like flies (dTOR), and mammals. In multicellular eukaryotes, there are two distinct complexes forming mTOR: mTOR complex 1 and 2 (mTORC1 and mTORC2). mTORC1 is a multiprotein complex consisting of the proteins mTOR, Regulatory-associated protein of mTOR (RAPTOR), MTOR associated protein LST8 homolog (MLST8), Proline-rich Akt substrate of 40 kDa (PRAS40) and DEP domain-containing mTOR-interacting protein (DEPTOR) (Wang & Zhang, 2019). The complex has several roles including cell growth and proliferation and the control of protein synthesis, as well as holding the primary

role in autophagy regulation (Yang & Klionsky, 2009). Less is known about mTORC2, but it is shown to have a promoting role in cell survival and cell cycle progression (Li et al., 2014). mTORC1 is activated in the case of nutrient-rich conditions, which causes inhibition of the autophagy process and activation of the mTOR pathway. Under nutrient deprivation, AMPK gets phosphorylated and activated by Liver kinase B1 (LKB1). This leads to suppression of mTORC1 either by phosphorylation and activation of Tuberous Sclerosis Complex 2/Tuberin (TSC2), which inhibits the mTOR activity, or by directly binding of AMPK to RAPTOR. This will activate the autophagy process. That is, autophagy is induced by starvation and is sensitive to availability of food and nutrients. There are several other regulatory signals which regulate mTORC1 in different ways, which will not be mentioned (Minnerly et al., 2017; Wang & Zhang, 2019).

In the case of nutrient deprivation, autophagy is essential to provide cellular energy to maintain cell survival (Noda & Ohsumi, 1998). The activation of the mTOR pathway regulates a group of downstream signaling pathways that control cellular proliferation, growth, motility, survival, and protein synthesis. On the other hand, the inhibition of this pathway is shown to extend the lifespan of model organisms like the nematode *C. elegans* (Zhang et al., 2020).

1.4.3 Autophagy in aging and disease

Studies using yeasts, worms, flies, and mice over the past decades have shown that during development and disease, autophagy plays crucial roles. In several conserved longevity paradigms, it is demonstrated that autophagy-related genes are required in the observed lifespan extension, indicating that autophagy plays a direct role in modulating aging. Interventions like dietary restrictions and treatment with rapamycin, which are shown to extend lifespan, are also shown to require an intact autophagic machinery, supporting that autophagy has a role in the maintenance of organismal homeostasis and extension of longevity. It is also shown that in most tissues, autophagy decline with age (Aman et al., 2021; Hansen et al., 2018).

Several different studies show a positive effect of increased autophagy on aging and age-related diseases (Aman et al., 2021). In several disease models, proteostasis collapse and proteotoxicity are suppressed by treatment with pharmacological autophagy inducers (Boland et al., 2018). In flies and cell culture, autophagy-increase led to suppressed toxicity from neurodegenerative disease-associated proteins (Berger et al., 2006). In the fruit fly *Drosophila,* treatment that increased autophagy resulted in a suppressed age-related protein aggregation as well as

extended lifespan (Schinaman et al., 2019). Neuronal and muscle stem cell function in aged mice have also shown to improve, and inhibition of age-related protein aggregation is seen by activation of autophagy (Audesse et al., 2019; García-Prat et al., 2016; Leeman et al., 2018). Even with only a few studies mentioned, there is great support that autophagy protects cells from toxic misfolded and aggregated proteins which in turn promotes healthy aging (Aman et al., 2021). In addition to laboratory models, human samples are also used in studies who show that autophagy is essential for suppression of age-associated inflammation, maintenance of homeostasis in tissues and cells, and maintenance of genomic integrity. The overall results are improved tissue health, increased lifespan, and embryonic development. Further studies on the link between autophagy and the other hallmarks of aging is necessary to better understand aging and disease and the molecular mechanisms behind (Aman et al., 2021).

1.4.4 The *C. elegans* autophagy protein ATG-18 and its mammalian homolog WIPI2

Autophagy-related protein 18 (ATG-18) is an autophagy protein with essential roles in autophagy and lifespan extension in *C. elegans* (Takacs et al., 2019). The protein is recruited by and bind to PI3P, recruit other proteins, and promotes formation and elongation of the phagophore (Minnerly et al., 2017).

A loss-of-function mutation can be initiated in the *atg-18* gene in *C. elegans*. The *C. elegans* null mutant *atg-18(gk378)* has this loss-of-function mutation (Minnerly et al., 2017), which is gathered by a functional 666 bp deletion in the *atg-18* gene coding for the ATG-18 protein (Takacs et al., 2019). This type of mutation will completely suppress autophagy in the organism, which will result in more protein aggregation, acceleration of the onset of age-related paralysis as well as shorten the lifespan (Aman et al., 2021). p62/SQSTM1 is a selective cargo receptor for degradation of protein aggregates by autophagy in *C. elegans*. Accumulation of p62/SQSTM1 is also an indicator of suppressed autophagy in the *C. elegans atg-18(gk378)* mutant. As this mutant is shown to have a shorter lifespan than the WT, Minnerly et al. did a study to investigate in which tissues *atg-18* expression is required to maintain the WT lifespan. ATG-18 is expressed in almost every tissue of the worm, but the results indicated that the autophagy activity, and hence the *atg-18* expression in neurons and intestinal cells is essential to maintain WT lifespan. They also found that an overexpression of *atg-18* in tissues where the gene is natively expressed in the WT worms decreased the WT lifespan. As previously

mentioned, nutrient deprivation (and thus dietary restriction) contributes to inhibition of mTOR, which in turn activates the autophagy process. Studies have showed that *C. elegans atg-18(gk378)* mutants do not show a response in lifespan extension to a dietary restriction, while *atg-18* worms with the *atg-18* gene in neurons or intestinal cells significantly restored the lifespan after dietary restriction treatment. This implies that ATG-18 is required for autophagy, which again is required for lifespan extension by dietary restriction (Minnerly et al., 2017; Takacs et al., 2019).

The WIPI protein family consists of proteins with roles in the autophagosome formation's early steps. The WIPI protein family consist of four proteins; WIPI1, WIPI2, WIPI3, and WIPI4, where WIPI1 and WIPI2 are mammalian homologs of the ATG-18 protein (Bakula & Scheibye-Knudsen, 2020). WIPI2B and WIPI2D promotes the recruitment of the ATG5-ATG12-ATG16L complex and the lipidation of LC3 in the autophagosomal membrane. This is done in a PI3P-dependent manner, a similar process to which is explained for ATG-18 in *C. elegans*. One implication that ATG-18/WIPI is evolutionarily conserved between humans and *C. elegans* is that WIPI proteins are involved in the pathogenesis of age-related diseases in humans, like neurodegenerative disorders and cancer. (Minnerly et al., 2017).

Studies on depletion and expression of WIPI in mammals show several of the same effects as in *C. elegans*. A study in aged mice showed that overexpression of WIPI2B in the neurons restored the rate of autophagosome biogenesis found in young adult mice (Stavoe et al., 2019). In humans, a lack of WIPI-expression and altered WIPI mutations is seen in many cancer types, and dysregulation of the human WIPI protein is a cause for neurodegeneration. Human WIPI proteins are also shown to have important functions in decoding the essential PI3P signal which initiates autophagy. These findings, in addition to the role of ATG-18 in *C. elegans* may indicate that WIPI proteins, with focus on the modulation of autophagy, can represent targets for new therapies within anti-aging (Grimmel et al., 2015).

1.5 Rapamycin

Rapamycin (Fig. 4), also known as Sirolimus, is a pharmacological agent and macrocyclic antibiotic with immunosuppressive effects (Hu et al., 2019). It was first discovered as an antifungal metabolite in the bacteria *Streptomyces hygroscopicus* in 1975 and was later introduced as an immunosuppressant for treatment of renal transplant in human patients (Li et

al., 2014). Rapamycin is a specific mTOR inhibitor which can trigger the same cell reaction as nutrient deprivation (Sabatini, 2017). In other words, rapamycin can induce autophagy in the cells even in the case of nutrient-rich conditions. By inhibiting mTOR and inducing direct autophagy, treatment with rapamycin can increase both lifespan and some healthspan parameters in worms, flies, and mice. Both the median and maximum lifespan of mice are shown to increase when treated with rapamycin late in life (Aman et al., 2021). Studies have shown that age-related protein aggregation is suppressed in mice and flies after treatment with rapamycin. The flies also showed extended lifespan in an autophagy-dependent manner after treatment. Toxicity from proteins associated with neurodegenerative diseases is suppressed in both cell culture and fly models, and by the induction of autophagy, rapamycin has shown contribution to protection against AD and other neurodegenerative diseases (Aman et al., 2021).

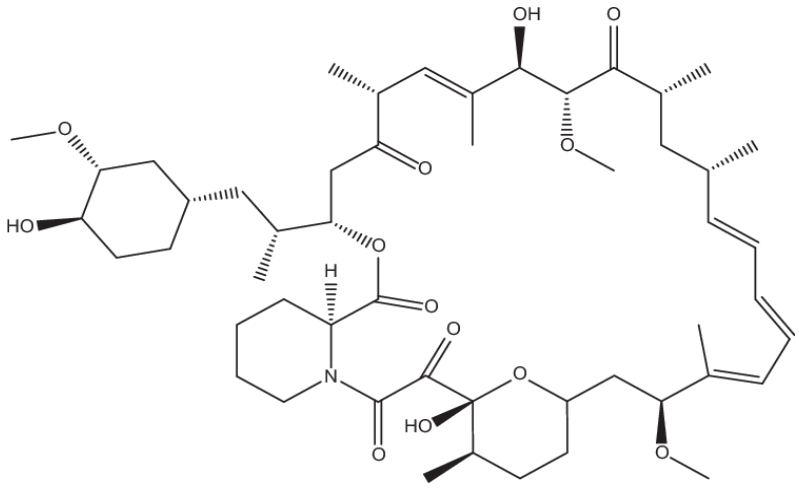

Figure 4. The structural model of rapamycin. *The figure is obtained from (Chrienova et al., 2021).*

Rapamycin is not a direct inhibitor of mTOR, but forms a complex with FKBP12, a 12 kDa FK506-binding protein. The FKBP12-rapamycin complex binds allosterically to a region immediately upstream of the catalytic domain of mTOR, and thereby inhibit the activity of mTOR. This allows the initiation of the autophagy process (Li et al., 2014). It was long thought that rapamycin only inhibits the functions of mTORC1, but recent studies have also shown indirect inhibition of the function of mTORC2 by rapamycin in long-term treated cells. Still, little is known about the mTORC2 upstream regulating signals compared to those of mTORC1 (Wang & Zhang, 2019).

1.6 Aims of the study

As aging is a biological process which affects most living organisms and increases the risk of several major human diseases, studies on aging can be beneficial not only to individuals, but also for societies in all parts of the world. A better understanding of the molecular mechanisms behind aging and age-related diseases is important for identifying pharmaceutical targets to develop treatment for age-related diseases, and also to improve human health during aging to minimize the global socioeconomic burden and challenges in healthcare (Aman et al., 2021; Lopez-Otin et al., 2013). The role of autophagy in aging and disease has been widely studied, and it is indicated that autophagy plays a direct role in modulating aging and that an increased rate of autophagy contributes to extended lifespan and "healthy aging" in several model organisms. Several studies have suggested that nutrient deprivation/starvation, or treatment with other interventions like rapamycin induces autophagy, and hence promotes extended lifespan.

As the autophagy-related protein ATG-18 has shown to be required for autophagy, the main aim of this study is to investigate the role of rapamycin in an *atg-18* mutant strain of *C. elegans* (*C. elegans atg-18(gk378)*), with a loss-of-function mutation in the *atg-18* gene. The study will explore whether rapamycin can affect lifespan and/or healthspan of *C. elegans* without the ability to induce autophagy. To achieve this, lifespan assays and different healthspan assays will be performed with rapamycin-treated *C. elegans atg-18(gk378)* mutants, as well as non-treated mutants, a WT strain of *C. elegans* (N2) with rapamycin-treatment, and a WT strain without rapamycin-treatment to investigate the potential differences.

As a supplement, a sub-aim of the study is to validate the effect of rapamycin on autophagy and the WIPI2B-protein in human cells. The aim of this is to validate if rapamycin influences WIPI2B and autophagy under conditions where autophagy can take place. To achieve this, HeLa cells with GFP-tagged WIPI2B will be treated with rapamycin, and live-images will be compared to see if the cells express more autophagy after rapamycin-treatment compared to both negative and positive control cells. Western Blots will also be performed to investigate whether the amount of several autophagy-related proteins increases in cells treated with rapamycin.

2 Materials

Overviews of the laboratory equipment, chemicals, antibodies, and software used in this study are found in **Appendix A** (**Table A.1**, **Table A.2**, **Table A.3**, **Table A.4** and **Table A.5**).

2.1 Strains

The two *C. elegans* strains used in this study were kindly provided by The Evandro Fang Lab. The wildtype (WT) strain used was N2. The mutant strain used to assess worms with a loss-of-function mutation in the *atg-18* gene was *C. elegans atg-18(gk378)* harboring a functional 666 bp deletion in the *atg-18* gene.

The cell line used in this study was HeLa GFP-WIPI2B. This is a HeLa cell line with green fluorescent protein (GFP)-tagged WIPI2B proteins, which are stably expressing GFP-WIPI2B. The cell line was generated by Professor Han-Ming Shen and Dr. Lu Guang in Professor Han-Ming Shen's lab at the Department of Physiology, Yong Loo Lin School of Medicine, National University of Singapore, and was kindly provided as a gift to the Evandro Fang Lab.

2.2 Buffers and other solutions

2.2.1 Running buffer

List of chemicals:

- NuPAGE™ MES SDS Running buffer (20X)
- dH_2O

50 mL of 20X NuPAGE™ MES SDS Running buffer was diluted in 950 mL dH_2O to obtain a 1X concentrated running buffer.

2.2.2 Transfer buffer

List of chemicals:

- NuPAGE™ Transfer Buffer (20X)
- dH_2O

- 100% Methanol (MeOH)

50 mL of 20X NuPAGE™ Transfer Buffer was diluted in 850 mL dH_2O to obtain a 1X concentrated transfer buffer. 100 mL of 100% MeOH was added to the solution to obtain a final concentration of 10% MeOH.

2.2.3 K-buffer

List of chemicals:

- 102.2 g KH_2PO_4
- 57.06 g K_2HPO_4
- ddH_2O

The dry reagents were weighed out, added to a 1 L glass bottle, and dissolved with ddH_2O to a final volume of 1 L. The bottle was then sterilized by autoclaving at 121°C for 20 minutes.

2.2.4 M9 buffer

List of chemicals:

- 3 g KH_2PO_4
- 6 g Na_2HPO_4
- 5 g NaCl
- 1 mL sterile 1 M $MgSO_4$
- ddH_2O

The dry reagents were weighed out, added to a 1 L glass bottle, and dissolved with ddH_2O to a final volume of 1 L. The bottle was then sterilized by autoclaving at 121°C for 20 minutes. After autoclaving and cooling down of the solution, 1 ml autoclaved/sterile 1 M $MgSO_4$ was added to the solution. The buffer was stored at room temperature until use.

2.2.5 Bleaching solution

List of chemicals:

- 28 mL ddH_2O

- 8 mL Chlorine
- 4 mL 5 M NaOH

Chlorine and 5M NaOH were mixed with ddH_2O in a 50 mL Falcon tube and stored at room temperature until use.

2.2.6 FUDR solution

List of chemicals:

- 15 mM Floxuridine (FUDR)
- ddH_2O

15 mM FUDR was stored at -20°C before use. The FUDR was taken out of the freezer and thawed. When thawed, the needed amount of FUDR and ddH_2O were mixed in a 1:4 ratio in a Falcon tube, resulting in a FUDR concentration of 75 μM.

2.2.7 Tris Buffered Saline Tween 20 (TBST)

List of chemicals:

- 100 mL 10X Tris Buffered Saline (TBS)
- 1 mL Tween 20
- 900 mL dH_2O

10X Tris Buffered Saline was diluted in dH_2O to make a 1X dilution of TBS before 1 mL of Tween 20 was added. The solution was stored in room temperature.

2.2.8 Milk-TBST solution

List of chemicals:

- 2.5 g Nonfat Dry Milk (#9999)
- 50 mL TBST (**2.2.7**)

Nonfat dry milk was weighted out and dissolved in TBST in a 50 mL Falcon tube to obtain a concentration of 5% milk-TBST solution. The solution was stored at 4°C.

2.3 Cultivation Medium and Agar

2.3.1 Nematode Growth Medium (NGM)

List of chemicals:

- 3 g NaCl
- 21 g agar
- 2.5 g peptone
- 200 mg/L streptomycin sulfate
- Up to 1 L dH_2O

The dry reagents were weighed out, added to a 1 L glass bottle, and dissolved in dH_2O to a final volume of 1 L. The bottle was then divided in two, resulting in two bottles with 500 mL NGM in each. The solution was then made sterile by autoclaving at 121°C for 20 minutes. Autoclaved NGM bottles were stored at 4°C until use.

2.3.2 Lysogeny Broth (LB)

Lysogeny Broth is a medium used for growth of OP50 bacteria.

The Lysogeny Broth used in this study was kindly provided by the Evandro Fang lab.

2.3.3 OP50

OP50 is an *Escherichia coli* mutant strain used as food for *C. elegans* (Félix & Braendle, 2010).

List of chemicals and equipment:

- OP50 colony (kindly provided by Evandro F. Fang)
- Lysogeny Broth (**2.3.2**)
- 50 mL Falcon tube
- Multitron Standard Shaker
- 100 mM Rapamycin
- DMSO

A single colony of OP50 was picked and added to a 50 mL Falcon tube containing 40 mL Lysogeny broth. The tube was incubated in a Multitron Standard Shaker at 200 rpm at 37°C overnight. The next day, the LB with OP50 was divided into two Falcon tubes, resulting in 20 mL in each. In one of the tubes, DMSO was added to a final concentration of 0.2%. In the other tube, rapamycin was added to a final concentration of 100 μM. This was done right before seeding onto the plates (**3.1.3**).

2.3.4 Cell growth medium

List of chemicals:

- 45 mL Dulbecco's Modified Eagle Medium (DMEM) with 4.5 g/L glucose with L-glutamine and sodium bicarbonate, without sodium pyruvate, without Hepes
- 5 mL Fetal Bovine Serum, Qualified (FBS)
- 500 μL Penicillin/Streptomycin (P/S)

To prepare the medium for growth and maintenance of the HeLa-cells, DMEM was mixed with FBS and P/S in a 50 mL Falcon tube under sterile conditions. The resulting medium should contain 10% FBS and 1% P/S. The medium was stored at 4°C until use. This amount of medium was made whenever needed.

2.4 Kits

Table 1. Kits*. The table gives an overview of the different kits used in this study, along with the contents and supplier of the kits.*

Kit	**Supplier**	**Contents**
Pierce™ BCA Protein Assay Kit	Thermo Scientific™	- BCA Reagent A, 2 x 500 mL - BCA Reagent B, 25 mL - Albumin Standard Ampules, 2 mg/mL, 10 x 1 mL
SuperSignal™ West Femto Maximum Sensitivity Substrate	Thermo Scientific™	- Luminol/Enhancer - Stable Peroxide Buffer

3 Methods

3.1 Preparation for experiments with *C. elegans*

3.1.1 Bleaching

Bleaching is a technique used for synchronizing *C. elegans* cultures. Worms are sensitive to bleach, but the embryos inside the eggs are protected by the eggshell. For this reason, bleaching can be performed on plates containing reproductive adult worms. The adult worms will die, while the eggs inside of the worms survive and ensures a culture of synchronized worms.

Materials:

- *C. elegans*, N2 and *atg-18(gk378)*
- Bleaching solution (**2.2.5**)
- M9 buffer (**2.2.4**)
- Glass pipette
- Heraeus Fresco 17 Centrifuge
- 1.5 mL Micro Tubes
- Vortex
- Petri plates, 100 mm

Method:

N2 and *atg-18(gk378)* worms were transferred from the NGM plates to separate Micro tubes using M9 buffer and a glass pipette. After some minutes, the worms were collected in the bottom and the supernatant was discarded. 1 mL of the bleaching solution was added to each tube, and the tubes were vortexed for about 5 minutes, until the destruction of the adult tissue. The tubes were then centrifuged at 17,000 g for 60 seconds, before the supernatant was discarded. The eggs were then washed by adding 1 mL M9 buffer to each of the tubes before they were centrifuged at 17,000 g for 60 seconds. The washing step was repeated three times. The eggs in the tubes were then placed onto 100 mm NGM agar plates with OP50 (made in the same procedure as in **3.1.3**) and incubated at 20°C until day 1 of adulthood.

3.1.2 Preparation of NGM agar plates

Materials:

- 500 mL prepared NGM (**2.3.1**)
- 500 µL 1 M $MgSO_4$
- 500 µL 1 M $CaCl_2$
- 500 µL (5 mg/mL EtOH) Cholesterol
- 12.5 mL K-buffer (**2.2.3**)
- 250 µL 100 mM Rapamycin
- 750 µL DMSO
- Petri plates, 60 mm
- Burning flame

Method:

The bottle with NGM kept at 4°C was melted in a microwave and then kept in a water bath at 55°C for approximately an hour prior to making the solution. In a relative sterile environment, close to a burning flame, $MgSO_4$, $CaCl_2$, Cholesterol and K-buffer were added to the bottle containing 500 mL NGM. The solution was mixed by swirling the bottle gently. The solution was then divided into two bottles, resulting in approximately 257 mL in each. 500 µL of DMSO was added and mixed into one of the bottles for making control plates. In the other bottle, a mix of 250 µL 100 mM rapamycin and 250 µL DMSO was added before the bottle was swirled gently to mix. From the respective bottles, 8 mL of mixed NGM-solution was added to each 60 mm petri plate, resulting in approximately 32 plates containing NGM-solution with 100 µM rapamycin, and 32 plates containing NGM-solution with 0.2% DMSO. The plates were left to dry in the dark, at room temperature for two days.

3.1.3 Seed NGM plates with OP50

Materials:

- NGM agar plates (**3.1.2**)
- OP50 with rapamycin (**2.3.3**)
- OP50 with DMSO (**2.3.3**)

Method:

After two days, the NGM agar plates prepared in **3.1.2** were seeded with OP50 (**2.3.3**). 200 µL of the OP50 with DMSO was seeded out on the prepared NGM agar plates with DMSO that

were going being used in the first days of the *C. elegans* experiments, while 100 µL was seeded out on the rest of the NGM agar plates with DMSO. The same was done for the NGM agar plates containing rapamycin, but these were seeded with OP50 containing rapamycin. The OP50 was seeded out in an even circle in the middle of the plates and left to dry in room temperature for two days before use. After two days, the first plates needed for the experiments were added FUDR (**3.1.4**). The plates that were to be used later in the experiment were stored upside down, wrapped with Parafilm®, in the dark at 4°C for up to 7 days.

3.1.4 Add FUDR to NGM plates

FUDR is a drug that controls the *C. elegans* population by inhibiting the DNA replication. This leads to a blocking of the effective reproduction by preventing the hatching of eggs, which in turn allows maintenance of synchronous *C. elegans* populations (Wang et al., 2019).

Materials:

- 75 µM FUDR (**2.2.6**)
- NGM plates with OP50 (**3.1.3**)

Method:

4-12 hours before use of the NGM plates (2 days after OP50 was added to the NGM plates), 200 µL of 75 µM FUDR was placed on each plate, drop by drop on and around the OP50 lawn using a pipette. The plates were then left to dry at room temperature before use.

3.2 Lifespan and healthspan assays with *C. elegans*

3.2.1 Transferring of worms for lifespan and healthspan assays

Materials:

- 60 mm NGM agar plates with OP50 and FUDR (**3.1.4**)
- Plates with synchronized *C. elegans* strains, both N2 and *atg-18*(*gk378*) (**3.1.1**)
- Worm picker (with platinum wire)

Method:

When both synchronized *C. elegans* populations reached day 1 of adulthood, the desired number of worms were transferred from the 100 mm NGM agar plates to prepared 60 mm NGM agar plates with OP50 and FUDR. Using a worm picker made with a glass pipette and a platinum wire, N2 and *atg-18*(*gk378*) worms were carefully transferred to one control plate (with DMSO) and one rapamycin plate each, resulting in four different treatment groups on four different plates: N2 control (Vehicle), N2 rapamycin, *atg-18*(*gk378*) control (Vehicle) and *atg-18*(*gk378*) rapamycin. These four treatment groups will hereafter be referred to as "different treatment groups".

3.2.2 Lifespan assay

Materials:

- 3 60 mm NGM agar plates with desired number of worms per treatment group (**3.2.1**)
- New NGM agar plates with OP50 and FUDR (**3.1.4**)
- Worm picker (with platinum wire)

Method:

The lifespan assay was done in three parallels (technical repeats), so the transferring described in **section 3.2.1** was done three times for each biological repeat of the lifespan assay resulting in three plates for each of the four treatment groups. 25-35 worms were transferred to each NGM plate when the worms reached day 1 of adulthood, which was the first day of the lifespan. From this day, all worms on all plates were counted every day. The number of dead, disappeared and appeared worms were noted each day during the whole lifespan. The worms were declared as dead when they failed to move in response to gentle prodding with the worm picker. Worms that died from desiccation on the edge of the plate or somehow disappeared were excluded from the data. On adult day 3 and 5, all worms were transferred to new NGM agar plates with OP50 and FUDR using a worm picker, to ensure they would not starve. Whenever a worm died, it was removed from the plate. Three biological repeats of the lifespan assay were performed during the study. The results were plotted in the "Rainbow Analyzer for *C. elegans* lifespan" excel-template made by Alexander Anisimov and Tomás Schmauck-Medina, where the graphs were made. The Log-rank (Mantel-Cox) test in GraphPad Prism 9 were used for the statistical analyzes.

3.2.3 Pharyngeal pumping assay

Materials:

- The same plates with worms used in the lifespan assay (**3.2.2**)
- Timer
- Counter
- Stemi 508 Microscope

Method:

The pumping assays were performed on day 4, day 8 and day 12 of the lifespans, meaning the worms were 4, 8 and 12 days into adulthood. The worms used in the pumping assays were the same as in the lifespan assays, meaning three parallels of the four different treatment groups per biological repeat. Using a timer and a manual counter, the pumping of 10 worms on each of the 12 plates was counted for 30 seconds each. One rhythmic contraction of the pharynx counted as one "pump" and was observed through the microscope. Three biological repeats of the pumping assay were performed during the study. The results were plotted in GraphPad Prism 9 where all plots and statistical analyzes were made. The statistical analyzes were done using Ordinary one-way ANOVA with Tukey's multiple comparisons test.

3.2.4 Thrashing assay

Materials:

- 2 60 mm NGM agar plates with desired number of worms per treatment group (**3.2.1**)
- New 60 mm NGM agar plates with OP50 and FUDR (**3.1.4**)
- Worm picker (with platinum wire)
- M9 buffer (**2.2.4**)
- Stemi 508 Microscope
- Microscope slide
- Automated pipette
- Timer
- Counter

Methods:

The transferring described in **section 3.2.1** was done two times in each biological repeat of the thrashing assay, resulting in two plates for each of the treatment groups per biological repeat. Two plates per group were prepared to ensure enough worms for the assay. 30 worms were transferred to each plate. The thrashing assay was performed on adult day 4, 6 and 8, and all worms on all plates were, using a worm picker, transferred to new NGM agar plates with OP50 and FUDR on days 3 and 5 to ensure they would not starve. A microscope slide was placed under the microscope and one drop M9 buffer was placed on the slide. Using a worm picker, one worm was carefully picked from the plate and placed in the M9 buffer. After allowing the worm to adapt for about 10 seconds, the thrashing of the worm was counted for 30 seconds. One thrash was counted as a bent of the body (head and/or tail) to one side and back to initial posture. After 30 seconds, the worm was discarded, and a new drop of M9 buffer and a new worm was placed on the microscope slide. Depending on the remaining number of worms on the plates, the thrashing of 7-20 worms from each group were counted on each day. Three biological repeats were performed on day 4, one biological repeat was performed on day 6, and two biological repeats were performed on day 8. The results were plotted in GraphPad Prism 9 where all plots and statistical analyzes were made. The statistical analyzes were done using Ordinary one-way ANOVA with Tukey's multiple comparisons test.

3.2.5 Worm sizer

Materials:

- 5 60 mm NGM agar plates with desired number of worms per treatment group (**3.2.1**)
- New NGM agar plates without OP50 (**3.1.2**)
- M9 buffer (**2.2.4**)
- Glass pipette
- Nikon Eclipse Ti2 Microscope with 4x objective
- 1.5 mL Micro Tubes

Method:

The transferring described in **section 3.2.1** was done five times to obtain five NGM agar plates with worms for each of the treatment groups. Five plates per group were prepared to ensure enough worms for the whole experiment. 30 worms were transferred to each plate. When the

worms reached day 3 of adulthood, all worms from all five plates from the same group were transferred to a Micro tube using M9 buffer and a glass pipette. When all worms were collected at the bottom of the tube, most of the supernatant was discarded. M9 buffer was added to wash the worms, and when all worms were collected at the bottom, the supernatant was discarded. The worms were transferred to a new NGM agar plate without OP50 using a glass pipette, and the plate was left to dry for some minutes. When dry, the plate was placed in a Nikon Eclipse Ti2 Microscope with a 4x objective and 19-37 worms per group were imaged. This was repeated for all four treatment groups.

The images were analyzed using the WormSizer software, a plugin for the ImageJ/Fiji (Fiji being a distribution of ImageJ with focus on analysis of biological images (Schindelin et al., 2012) software, which provides an automated analysis of nematode size and shape (Moore et al., 2013). The output results from WormSizer were plotted in GraphPad Prism 9, where all graphs and statistical analyzes were made. The statistical analyzes were done using Ordinary one-way ANOVA with Tukey's multiple comparisons test.

3.3 Cell maintenance

3.3.1 Thaw cells

Materials:

- Frozen HeLa GFP-WIPI2B cells
- Cell growth medium (**2.3.4**)
- Heraeus Multifuge 1S-R Centrifuge
- Leica DMIL Microscope
- Sterile T75 tissue culture flask
- 15 mL Falcon tube
- Automated pipettes

Method:

The cells used in this study were kept at -150°C. The tube with frozen cells was put in a 37°C water bath to start the melting process. Then 37°C growth medium was added directly to the cells in the tube to melt the freezing solution (DMSO). When the solution with the cells was melted, it was transferred to a 15 mL Falcon tube containing 10 mL growth medium and

centrifuged at 1200 rpm for 3 minutes. After centrifugation, all cells were collected in the bottom of the tube. The supernatant was removed, 13 mL of new growth medium was added, and the cells were resuspended in the medium by pipetting up and down resulting in a homogenous single-cell solution. The medium with cells from the tube was then transferred to a sterile T75 tissue culture flask with filter cap. The cells were kept in a 37°C incubator for maintenance.

3.3.2 Splitting cells

Splitting of the cells kept in the tissue culture flask was done regularly during the study (every 3-4 days) to ensure cell growth. A failure to do this regularly will lead to overgrowth of the cells, which in turn can lead to stress and starvation of the cells.

Materials:

- HeLa cells in T75 tissue culture flask maintained at 37°C
- Cell growth medium (**2.3.4**)
- 0.05% Trypsin-EDTA (1X)
- Phosphate-buffered saline (PBS)

Method:

In a sterile hood, all the growth medium in the tissue culture flask was removed while the cells remained attached to the surface of the flask. To wash remaining medium off the cells, 10 mL of PBS was added to the flask (not directly on the cells) and removed again. Then, 1 mL of 0.05% Trypsin-EDTA was added directly to the cells to detach them from the surface. Ensured the trypsin covered the entire surface before the flask was incubated at 37°C for 3-5 minutes. After incubation, approximately 10 mL of new growth medium was added to the flask and pipetted up and down to ensure single cell suspension and not clusters of cells. Then, most of the medium with cells was removed. The amount saved was determined by how far in the future the cells would be used and varied from 1:5 to 1:20. 10-15 mL of medium was then added to the flask, before ensuring that the cells were equally divided in the flask using a microscope. The cells were then incubated at 37°C.

3.4 Cell treatment for Western Blotting and imaging

3.4.1 Find appropriate number of cells for experiments

For imaging-experiments with cells, it is important to use an appropriate number of cells. An appropriate number of cells is the amount where there are some space between the cells, but not too much. The confluence, which describes the density of the cells, should be around 70-80%. To find the appropriate number of cells for the experiments, the cells were counted and seeded out in different amount in different wells.

Materials:

- HeLa cells in T75 tissue culture flask maintained at 37°C
- Cell growth medium (**2.3.4**)
- 0.05% Trypsin-EDTA (1X)
- PBS
- Heraeus Multifuge 1S-R Centrifuge
- 15 mL Falcon tubes
- Hemocytometer
- Leica DMIL Microscope
- 6-well Tissue Culture plate
- Automated pipette

Method:

Before counting the cells, they were detached from the surface of the tissue culture flask. This was done in a sterile hood following the protocol for splitting cells described in **section 3.3.2**. After detaching the cells, all the medium with cells was added to a 15 mL Falcon tube and spinned down in a centrifuge at 1200 rpm for 3 minutes. After centrifugation, all cells were collected at the bottom of the tube, and the supernatant containing medium and trypsin was removed. 10 mL of new medium was added, and the cell pellet was resuspended using a pipette. 10 µL of the medium with cells was added to a hemocytometer and placed under a microscope. All cells in the four 16-squares in the hemocytometer were counted, and calculations were done to find the number of cells/mL in the solution. To calculate this number, the average number of cells in the four squares were found. This average was then multiplied by 10^4, resulting in the number of cells/mL. To find the appropriate number of cells to use for the experiments, 30,000, 40,000, 50,000, 60,000, 70,000, and 80,000 cells were seeded out in 6 different wells in a 6-

well plate. To calculate the amount of solution corresponding to these numbers of cells, the desirable number of cells was divided by the calculated number of cells/mL. 2 mL of growth medium was added to each of the 6 wells before the calculated amount of medium with desirable number cells were added to the designated wells. The 6-well plate was then incubated at 37°C for two days. After two days, the 6-well plate was put on a microscope to check which well had an appropriate number of cells to use for the future experiments.

3.4.2 Seed out cells

Materials:

- HeLa cells in T75 tissue culture flask maintained at 37°C
- Cell growth medium (**2.3.4**)
- 0.05% Trypsin-EDTA (1X)
- PBS
- Heraeus Multifuge 1S-R Centrifuge
- 15 mL Falcon tubes
- Hemocytometer
- Leica DMIL Microscope
- 6-well Tissue Culture plate

Method:

To prepare cell extracts for Western Blotting, 80,000 cells were seeded out in three different wells in a 6-well plate. This was done following the protocol for finding the appropriate number of cells for experiments described in **section 3.4.1**, but instead of doing calculations to find the amount of medium with cells corresponding to different numbers of cells, only the calculation for 80,000 cells was done. 2 mL of growth medium was added to three different wells in the 6-well plate, and the calculated amount of medium with cells was added to the medium in each well. The 6-well plate was then incubated at 37°C for two days. Three biological repeats were performed during the study.

3.4.3 Treatment and harvesting of cells

Materials:

- 6-well plate containing 80,000 cells x3 (**3.4.2**)
- Cell growth medium (**2.3.4**)
- PBS
- DMSO
- 100 mM rapamycin
- Earle's balanced salt solution (EBSS)
- Pierce™ RIPA buffer
- 100X Protease + phosphatase inhibitor cocktail
- Cell scraper
- Heraeus Fresco 17 Centrifuge
- 1.5 mL Micro Tubes
- Automated pipettes

Method:

After the two-days incubation of the 6-well plate (**3.4.2**), the medium in all three wells was removed. 2 µL DMSO was added to 2 mL of growth medium, and this solution was added to one of the wells now containing the Vehicle cells (negative control). 1 µL of 100 mM rapamycin was diluted in 1 mL DMSO to obtain a concentration of 100 µM rapamycin. 2 µL of this solution was added to 2 mL growth medium, which then was transferred to another well in the plate. The last well was washed 2x with 2 mL EBSS, before 2 mL EBSS was added to the well. Treatment with EBSS causes starvation of the cells and was used as a positive control. The 6-well plate was then incubated at 37°C for 2 hours.

During incubation, 200 µL RIPA buffer and 2 µL 100X protease + phosphatase inhibitor cocktail were mixed in a Micro tube on ice. After 2 hours incubation of the 6-well plate, the medium was removed from all three wells before they were washed with 2 mL PBS. 50 µL of the RIPA + 1X protease + phosphatase inhibitor cocktail mix was added to each well before the wells were scraped with a cell scraper. The scraped liquid now containing the cells in each well were transferred to separate Micro tubes using a pipette and incubated on ice for 30 minutes. Then, the tubes were centrifuged at 17,000 g at 4°C for 10 minutes. The supernatant was then

transferred to new Micro tubes on ice and kept at -80°C until use. This was done for all three biological repeats.

3.4.4 Cell imaging

Materials:

- HeLa cells in T75 tissue culture flask maintained at 37°C
- Cell growth medium (**2.3.4**)
- 0.05% Trypsin-EDTA (1X)
- PBS
- DMSO
- 100 mM rapamycin in DMSO
- Earle's balanced salt solution (EBSS)
- Heraeus Multifuge 1S-R Centrifuge
- 15 mL Falcon tubes
- Hemocytometer
- Zeiss Confocal LSM 780 microscope
- IBIDI glass bottom dishes

Method:

Following the protocol for finding the appropriate number of cells for experiments (**3.4.1**), calculations for finding the amount of medium containing 100,000 cells were made, and 100,000 cells were added to 2 mL growth medium in three different IBIDI glass bottom dishes. The dishes were then incubated at 37°C until the next day. After incubation, the cells were treated respectively with DMSO, rapamycin and EBSS for 2 hours as described in **section 3.4.3**. After incubation the cells were live-imaged with a Zeiss Confocal LSM 780 microscope with 40X oil objective imaging the GFP-signal. The GFP-signal corresponded to GFP-WIPI2B protein expressed in the HeLa cell line used. 10-16 images were taken per plate. After imaging, the cells treated with rapamycin were incubated over night at 37°C and imaged again 24 hours after treatment.

3.4.5 Analyzing images

The images of the cells after treatment with DMSO, EBSS and rapamycin were analyzed using the ImageJ software and GraphPad Prism 9 software. The mean intensity of GFP of each cell was found using ImageJ, and the mean intensity was used for quantification. ImageJ was also used to count the number of foci in each cell. The average number of foci per cell in each image was calculated. GraphPad Prism 9 was used to analyze the results for intensity and foci. GraphPad Prism 9 used Ordinary one-way ANOVA with Dunnett's multiple comparisons test to compare the results for each group and calculate the statistical differences. GraphPad Prism 9 were also used to make the graphs.

3.5 Protein concentration measurement

The Pierce^{TM} BCA Protein Assay Kit used in the following sections were used to determine protein concentration in the samples with the BCA Protein Assay. The assay is based on and combines the Cu^{2+} to Cu^{1+} reduction by protein in alkaline medium with the calorimetric detection of Cu^{1+} by bicinchoninic acid (BCA). The reactions develop a colored BCA/copper complex. At 562 nm, this complex expresses a strong linear absorbance with increasing protein concentrations (Thermo Fisher Scientific Inc). This absorbance can be measured in an ELISA reader.

3.5.1 Making standards

Materials:

- Pierce^{TM} BCA Protein Assay Kit
    - Albumin Standard Ampules (2 mg/mL)
- 1.5 mL Micro tubes
- Nuclease-Free water (NFW)

Method:

40 µL undiluted Albumin Standard was added to a Micro tube (Standard 1). In a new Micro tube, 40 µL NFW was mixed with 40 µL of Standard 1 to make Standard 2. This procedure was continued, resulting in a serial dilution made following **Table 2**.

***Table 2**. The table shows how to make the serial dilution of the New England BSA (2.0μg/μL).*

Standard	Concentration	Content
Standard 1	2.0 μg/μL	40 μL Albumin Standard (undiluted, 2.0 μg/μL)
Standard 2	1.0 μg/μL	40 μL NFW + 40 μL Standard 1
Standard 3	0.5 μg/μL	40 μL NFW + 40 μL Standard 2
Standard 4	0.25 μg/μL	40 μL NFW + 40 μL Standard 3
Standard 5	0.125 μg/μL	40 μL NFW + 40 μL Standard 4
Standard 6 (Blank)	0	40 μL NFW

3.5.2 Preparation for ELISA

Materials:

- Pierce™ BCA Protein Assay Kit
    - BCA Reagent A
    - BCA Reagent B
- 96-well Microplate
- Standard 1-6 **(3.5.1)**
- Samples of cell extracts (**3.4.3**)
    - 3 replicates of HeLa GFP-WIPI2B Vehicle
    - 3 replicates of HeLa GFP-WIPI2B treated with EBSS for 2h
    - 3 replicates of HeLa GFP-WIPI2B treated with rapamycin for 2h

Method:

10 μL of each standard 1-6 from **section 3.5.1** were added to the designated wells in a 96-well microplate in triplicates. The cell extracts kept at -80°C were thawed on ice before each cell extract sample were added to designated wells in a 10x dilution by mixing 1 μL of the sample with 9 μL NFW in triplicates. A mix of Pierce™ BCA Protein Assay Reagents A and B was made in a 50:1 ratio by adding 192 μL of reagent B to 9.6 mL of reagent A. 200 μL of this mix was then added to each well containing sample using a multichannel pipette. The solutions in

each well were mixed by pipetting up and down three times before the 96-well microplate was incubated in the dark at 37°C for 30 minutes.

3.5.3 ELISA

Materials:

- ELISA reader: Varioskan, version 3.01.15
- Prepared 96-well microplate with samples and standards (**3.5.2**)

Method:

The 96-well microplate with the samples and standards was read in an ELISA reader. The ELISA reader was set to a measurement time of 100 ms, measurement wavelength of 562 nm, and bandwidth of 5 nm. The results were exported to an Excel template, and for each sample, the amount of sample corresponding to 15-25 μg of protein was calculated based on the concentration of the cell supernatant.

3.6 Western Blotting

Western Blotting is a technique used to visualize and identify specific proteins of interest from a complex protein-mixture. Ahead of the Western Blotting, the mixture of proteins is separated through Sodium Dodecyl Sulfate-Polyacrylamide Gel Electrophoresis (SDS-PAGE), which separates proteins based on their molecular weight. After the separation, the proteins are transferred from the gel to a membrane. The membrane is then blocked to avoid unspecific binding, and then incubated with primary antibodies specific for the target protein. Secondary antibodies will bind to the primary antibodies and are contributors to the detection process. The amount of protein present in the sample corresponds to the thickness of the band after the visualization (Mahmood & Yang, 2012).

3.6.1 Sample preparation

Materials:

- Samples of cell extracts in RIPA buffer (**3.4.3**)

    - 3 replicates of HeLa GFP-WIPI2B Vehicle
    - 3 replicates of HeLa GFP-WIPI2B treated with EBSS for 2h
    - 3 replicates of HeLa GFP-WIPI2B treated with rapamycin for 2h
- NuPAGE™ LDS Sample Buffer (4X) (Loading dye)
- 1 M Dichlorodiphentyltrichloroethane (DDT)
- dH_2O
- 1.5 mL Micro tubes
- Stuart SBH130D Block heater

Method:

For all samples, the amount of sample corresponding to 15-25 µg of protein was used in the preparation for Western Blotting. The amount needed for each sample was calculated in an Excel template. A standard curve was made using the mean values of the standards from the results of the ELISA reader and the corresponding BSA concentration (from **Table 2**). For each sample, the y-intercept of the standard curve was subtracted from the mean value, and the difference was divided by the slope. This number was then multiplied by 10 due to the dilution of the samples during the measurement, and the result was the amount of sample that corresponded to 15-25 µg/µL of protein. The samples were mixed with dH_2O and NuPAGE™ LDS Sample Buffer (4X) + DDT. A total amount of 75 µL of this solution per tube was desirable, so 75 was divided by the calculated amount of sample to get the exact amount of sample to be added. In a hood, 2 µL of 1 M DDT was mixed with 198 µL of NuPAGE™ LDS Sample Buffer (4X). This solution was then added to the tubes in a 1:4 ratio, before water was added. The tubes were boiled at 97°C for 2 minutes in the Block heater before they were kept at -20°C until use.

3.6.2 SDS-PAGE

Materials:

- 1X Running buffer (**2.2.1**)
- NuPAGE™ 4-12% Bis-Tris Midi Gel
- Precision Plus Protein™ Kaleidoscope™ Prestained Protein Standards #1610375
- Prepared samples (**3.6.1**)
- SureLock™ Tandem Midi Gel Tank

- Syringe

Method:

The comb and tape were removed from two gels before they were placed in the SureLock™ Tandem Midi Gel Tank. 1X running buffer was used to fill the inner chamber of the tank such that the gel wells were submerged with buffer, and the outer chamber of the tank was filled to the marked fill line. The wells were then rinsed one time using a syringe filled with running buffer. 5 µL of the protein standard was loaded into two of the wells, before 14 µL of each sample were loaded in their designated wells. When all ladders and samples were loaded, the lid was placed on the tank, and the electrode cords were plugged into the power supply. The power supply was turned on and set to run at 200 V for 45 minutes.

3.6.3 Transferring proteins from gel to membrane

Materials:

- 1X Transfer buffer (**2.2.2**)
- 100% Methanol
- SureLock™ Tandem Tray
- SureLock™ Tandem Midi Blot Module
    - Sponge pad x2
    - Filter paper x4
    - Polyvinylidene difluoride (PVDF) transfer membrane
    - Gels from **section 3.6.2**
- Blotting roller

Method:

Everything in this section were done twice, since two gels were used in the gel electrophoresis. Inside a hood, the PVDF membrane was covered with 100% methanol to ensure the activation of the transfer membrane. It was important to make sure to never let the membrane dry out after this step. 1X transfer buffer was used to soak the sponge pads in the front compartment of the SureLock™ Tandem Tray, and a blotting roller was used to ensure that all air bubbles were removed. The gel chamber from **section 3.6.2** was opened, and the gel was carefully taken out and prepared for transferring by trimming off the foot and well fingers from the gel. The Blot

Module was placed into the back compartment of the tray, and 50 mL 1X transfer buffer was added to the cathode shell. The transfer stack was assembled by first placing a sponge pad on the cathode core. On top of the sponge pad, two filter papers soaked in 1X transfer buffer were placed, followed by the gel oriented with the wells toward the bottom of the Blot Module. The membrane was placed on top of the gel, and two soaked filter papers on top of the membrane. On the top, closest to the anode core, the second sponge pad was placed. During the assembly of each layer in the stack, the blotting roller was used to ensure all air bubbles were removed. Then, the Blot Module was closed and placed in the tank before the tank was filled with 1X transfer buffer to the fill line. The lid was placed on the tank, and the electrode cords were plugged into the power supply. The power supply was turned on and set to run at 25 V for 30 minutes.

3.6.4 Antibody incubation

Materials:

- 5% Milk-TBST solution (**2.2.8**)
- TBST (**2.2.7**)
- Primary antibodies from **Appendix A, Table A.3**
- Secondary antibodies from **Appendix A, Table A.4**
- Scalpel
- Falcon tubes
- Mini Rocker Shaker
- Roller mixer
- Small boxes

Method:

When the proteins were transferred from the gel to the membrane, the Blot Module was opened, and the membrane taken out and kept covered in TBST. The membrane was cut with a scalpel to get one piece of membrane for each protein of interest before the membranes were blocked in 5% milk-TBST solution for 1 hour at room temperature. During the incubation, primary antibodies were prepared by diluting them in milk-TBST solution in clean Falcon tubes. Each tube was prepared with the proper primary antibody for each of the protein of interest. The primary antibodies used are described in **Appendix A, Table A.3**. After the blocking, the

membranes were added to their respective tubes with the active side of the membrane pointing against the inside of the tube. The tubes were then incubated on a roller mixer at 4°C until the next day.

After the incubation, the membranes were washed in TBST in clean boxes and the boxes were then placed on a Mini Rocker Shaker for 10 minutes to wash away non-specific bound antibodies from the membrane. The TBST was drained out, new TBST was added, and the washing step was repeated 2 times. After a total of three washes, new 50 mL Falcon tubes were prepared by adding secondary antibodies and milk-TBST solution in a 1:3000 ratio. The secondary antibodies used are described in **Appendix A, Table A.4**. The membranes were incubated with the proper secondary antibody depending on the previous added primary antibody and incubated on a roller mixer for 1 hour. After incubation, the membranes were washed 3 times in TBST on a Mini Rocker Shaker as described above.

3.6.5 Western Blotting

Materials:

- Membranes from **section 3.6.4**
- SuperSignal™ West Femto Maximum Sensitivity Substrate
    - Luminol/Enhancer
    - Stable Peroxide Buffer
- ChemiDoc XRS+ Imaging System
- Plastic sheet
- 15 mL Falcon tube

Method:

In a 15 mL Falcon tube, Luminol/Enhancer and Stable Peroxide Buffer were mixed in a 1:1 ratio in a volume enough for approximately 500 µL per membrane. The tube was then covered in aluminum to protect it from light. The ChemiDoc XRS+ Imaging System was used for the detection. A thin plastic sheet was put in the system, and a membrane was put on top of the sheet with the active side facing upwards. Then the membrane was covered with the Luminol/Enhancer/Stable Peroxide Buffer mix before the membrane was detected and imaged using the Image Lab software from Bio-Rad and the standard protocol for chemiluminescence. The software was set to automatic determine the detection time based on high intensity bands

on the blot. After detection, the membrane was removed, and a new membrane was placed in the system.

3.6.6 Analyzing Western Blot results

The ImageJ software was used for quantification of the detected Western Blots. The results for each band from the Western Blot was divided by the corresponding band of β-Actin, which was used as the household protein. The fold change compared to Vehicle was found by dividing the result for the protein of interest in cells treated with rapamycin and EBSS divided by β-actin on the average Vehicle result. The fold change compared to Vehicle for each group and protein were plotted in GraphPad Prism 9 and analyzed using Ordinary one-way ANOVA with Dunnett's multiple comparisons test to compare the results for each group and calculate the statistical differences. The graphs were also made in GraphPad Prism 9.

4 Results

4.1 The effects of rapamycin on lifespan and healthspan in *C. elegans atg-18(gk378)* mutants

The effects of rapamycin on lifespan and healthspan in *C. elegans* mutants with a functional deletion of the essential autophagy-gene *atg-18* were investigated by comparing a rapamycin-treatment group with a group without treatment as well as to a WT strain (N2) of *C. elegans* with and without rapamycin treatment. The treatment groups were grown on NGM-agar plates containing 100 μM rapamycin in the NGM and 100 μM rapamycin in the OP50 (food), and the control groups were grown on NGM-agar plates containing 0.2% DMSO in the NGM and 0.2% DMSO in the OP50. The *C. elegans atg-18(gk378)* mutants will hereafter be called "mutants".

4.1.1 The effects of rapamycin on lifespan in *C. elegans atg-18(gk378)* mutants

The lifespan assays were performed to estimate the number of days the different groups of worms lived (counted from day 1 of adulthood). The results of the assay were plotted in the "Rainbow Analyzer for *C. elegans* Lifespan" excel-template, where the graphs were made. The statistical analyzes were done in GraphPad Prism 9 using the Log-rank (Mantel-Cox) test, **** $p \leq 0.0001$, *** $p \leq 0.001$, ** $p \leq 0.01$, * $p \leq 0.05$ and (ns) $p > 0.05$.

The *atg-18* gene is essential for maintenance of WT lifespan. The lifespan of the mutants in the control groups were significantly decreased compared to the WT lifespan in all biological repeats (**Fig. 5A-C,** and **Appendix B, Table B.1-B.3**) ($p \leq 0.0001$). The rapamycin-treatment of WT worms showed no significant difference compared to control WT (**Fig. 5A-C**). In the mutants, a significant decrease in lifespan is shown for the group treated with rapamycin compared to the mutants in the control group. All biological repeats showed this difference, with a variation in the degree of significance (**Fig. 5A**, $p \leq 0.0002$), (**Fig. 5B**, $p = 0.0445$), (**Fig. 5C**, $p = 0.0006$).

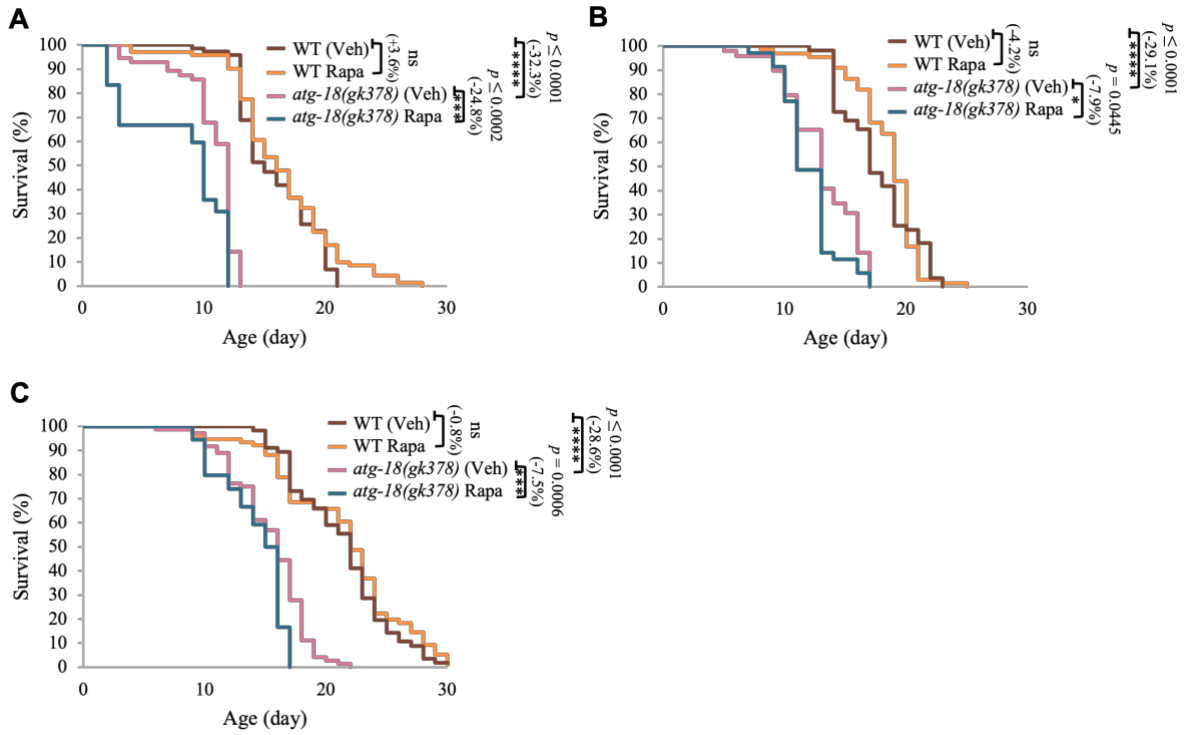

Figure 5. Effects of rapamycin on lifespan in C. elegans atg-18(gk378) mutants. *No significant difference in lifespan is shown between WT C. elegans with or without rapamycin treatment in the 1st biological repeat (A), The 2nd biological repeat (B), or the 3rd biological repeat (C). In all biological repeats (A-C), lifespan is significantly ($p \leq 0.0001$) decreased in the mutants compared to the WT (both without treatment). The lifespan of the mutants is significantly reduced by treatment with rapamycin in both 1st, 2nd, and 3rd biological repeat ($p \leq 0.0002$, $p = 0.0445$ and $p = 0.0006$, respectively). 35-76 worms per group, per biological repeat were included in the lifespan assay. The Log-rank (Mantel-Cox) test was used for the statistical results.*

4.1.2 The effects of rapamycin on pumping rate in *C. elegans atg-18(gk378)* mutants

The pumping assay was performed to investigate the effects of rapamycin treatment on the pharyngeal pumping of the mutants. The results were plotted in GraphPad Prism 9 where all plots and statistical analyzes were made. The statistical analyzes were done using Ordinary one-way ANOVA with Tukey's multiple comparisons test, **** $p \leq 0.0001$, *** $p \leq 0.001$, ** $p \leq 0.01$, * $p \leq 0.05$ and (ns) $p > 0.05$.

The results show that the pumping rate is significantly decreased from WT to mutants without treatment on both day 4, 8, and 12 (**Fig. 6A-C**) ($p \leq 0.0001$) showing that the mutation decreases this healthspan parameter in *C. elegans*. Comparisons between the WT control group and rapamycin-treated WT shows a significantly increase in the treated group on day 4 (**Fig. 6A**)

(p = 0.0216), a non-significant difference on day 8 (**Fig. 6B**), and a significant decrease in the treated group on day 12 (**Fig. 6C**) ($p \leq 0.0001$). For the mutant groups, there was so significantly difference in pumping rate between the rapamycin-treated group and the control group on days 4 (**Fig. 6A**) and 12 (**Fig. 6C**). On day 8 on the other hand, the pumping rate of the rapamycin-treated mutant group was significantly decreased compared to the control mutant group (**Fig. 6B**) (p = 0.0138). All groups showed a decline in pumping rate with age, and the mutant groups pumped slower than the WT groups on all tested days (**Fig. 6A-C**).

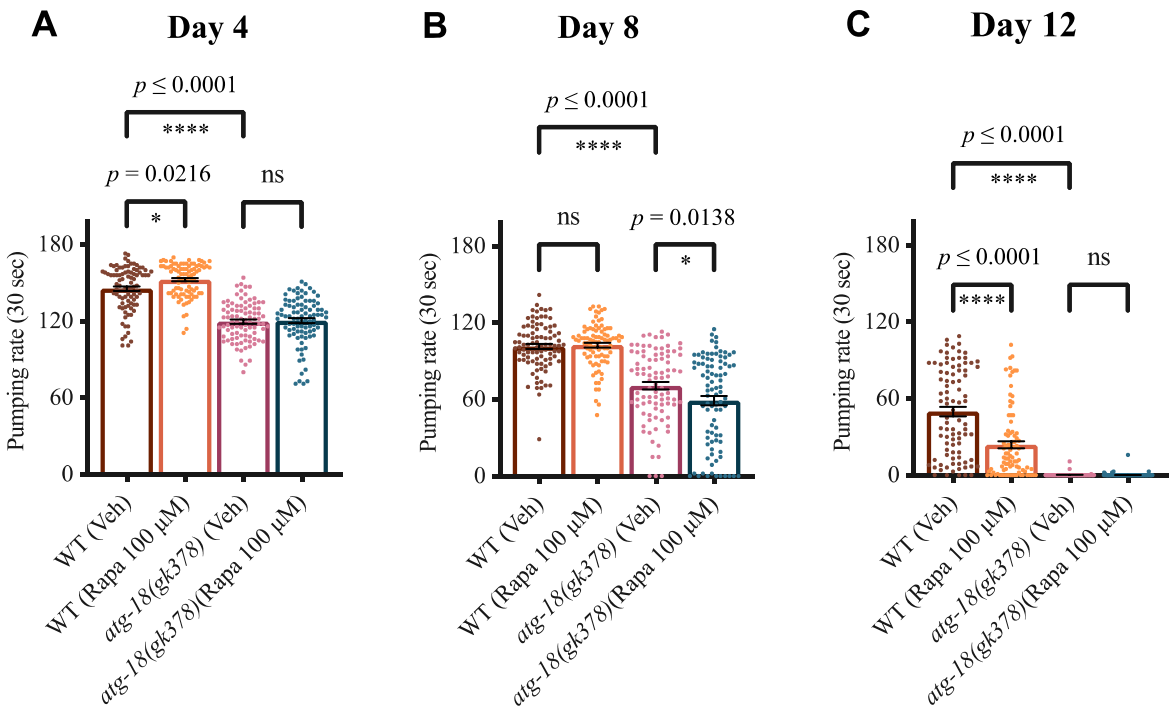

Figure 6. The effects of rapamycin on pharyngeal pumping in C. elegans atg-18(gk378) mutants. *The atg-18 mutation decreases the pumping rate in C. elegans on day 4 (A), day 8 (B), and day 12 (C) of adulthood significantly ($p \leq 0.0001$). On adult day 4 (A), there is a significant increase (p = 0.0216) in pumping rate in rapamycin-treated WT compared to non-treated WT, and no significant difference between treated and non-treated mutants. On adult day 8 (B), there are no significant difference between WT with or without treatment, but a significantly decrease (p = 0.0138) in rapamycin-treated mutants compared to non-treated mutants. On adult day 12 (C), there is a significant decrease ($p \leq 0.0001$) in pumping rate in rapamycin-treated WT compared to non-treated WT, and no significant difference between treated and non-treated mutants. The pumping of 30 worms per group were counted each day. Ordinary one-way ANOVA with Tukey's multiple comparisons test was used for the statistical results. The error bars are the standard error of the mean.*

4.1.3 The effects of rapamycin on thrashing rate in *C. elegans atg-18(gk378)* mutants

The thrashing assay was performed to measure the effects of rapamycin on the thrashing (swimming) rate of the *C. elegans* mutants. The results were plotted in GraphPad Prism 9 where all plots and statistical analyzes were made. The statistical analyzes were done using Ordinary one-way ANOVA with Tukey's multiple comparisons test, **** $p \leq 0.0001$, *** $p \leq 0.001$, ** $p \leq 0.01$, * $p \leq 0.05$ and (ns) $p > 0.05$.

The results shows that on day 4 (**Fig. 7A**) and day 6 (**Fig. 7B**), a significant decrease ($p \leq 0.0001$) in thrashing rate is shown for non-treated mutants compared to the non-treated WT. On day 8 on the other hand, this difference is not shown. On all tested days, WT worms with rapamycin treatment have a significantly higher thrashing-rate than WT worms without treatment, with $p = 0.0008$ on day 4 (**Fig. 7A**), $p = 0.0079$ on day 6 (**Fig. 7B**), and $p = 0.0052$ on day 8 (**Fig. 7C**). For the mutant groups, rapamycin-treatment seems to increase the thrashing rates on all tested days, but only the difference on day 4 is significant ($p = 0.0145$), while the differences on day 6 and 8 are not significant.

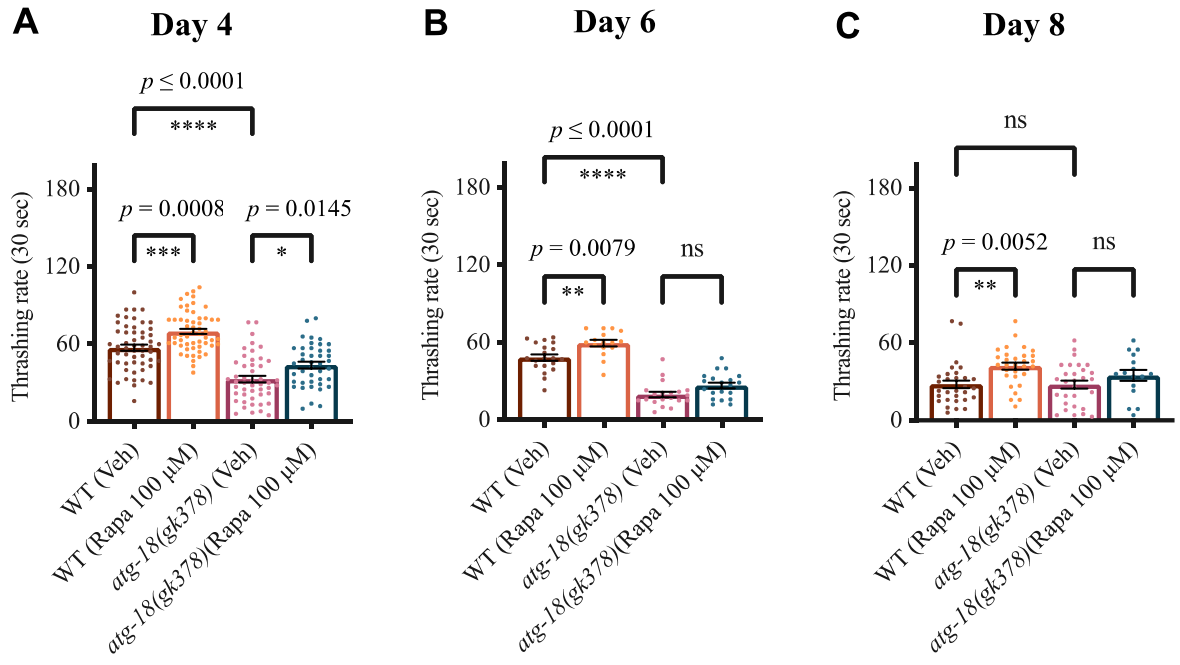

Figure 7. The effects of rapamycin on thrashing rate in C. elegans atg-18(gk378) mutants. *The atg-18 mutation significantly decreases ($p \leq 0.0001$) the thrashing rate on days 4 (A) and 6 (B), but not on day 8 (C). Rapamycin-treatment in WT worms significantly increases the thrashing rate on day 4 (A) ($p = 0.0008$), day 6 (B) ($p = 0.0079$), and on day 8 (C) ($p = 0.0052$). Rapamycin-treatment in the mutants significantly increases ($p = 0.0145$) the thrashing rate on day 4 (A), but not on day 6 (B) or 8 (C). Ordinary one-way ANOVA with Tukey's multiple comparisons test was used for the statistical results. The error bars are the standard error of the mean.*

4.1.4 The effects of rapamycin on the body size of *C. elegans atg-18(gk378)* mutants

As an interesting addition to the lifespan and healthspan assays, different size parameters of the worms were examined to see whether treatment with rapamycin showed any effects in the body size of the mutants compared to the WT. The resulting images were analyzed in WormSizer, and the results from WormSizer were plotted in GraphPad Prism 9 where all plots and statistical analyzes were made. The statistical analyzes were done using Ordinary one-way ANOVA with Tukey's multiple comparisons test, **** $p \leq 0.0001$, *** $p \leq 0.001$, ** $p \leq 0.01$, * $p \leq 0.05$ and (ns) $p > 0.05$.

The results show no significant difference between the treated and non-treated mutants on either volume (**Fig. 8A**), length (**Fig. 8B**), mean width (**Fig. 8C**), middle width (**Fig. 8D**) or surface area (**Fig. 8E**). Comparisons between WT with and without treatment only shows a significant difference in length, where WT without treatment is significantly ($p = 0.0145$) longer than WT with treatment (**Fig. 8B**). Interestingly, in all size parameters except middle width, the *atg-18* mutation decreases the body size compared to the WT (**Fig. 8A, B, E**) ($p \leq 0.0001$), (**Fig. 8C**) ($p = 0.0108$). The comparison of middle width and length, also shows that the mutants are smaller than the WTs, but it shows no clear difference between treated and non-treated groups (**Fig. 8F**). The results do not clearly indicate that rapamycin influences the body size of *C. elegans*, but they show that the mutants are clearly smaller than the WT worms.

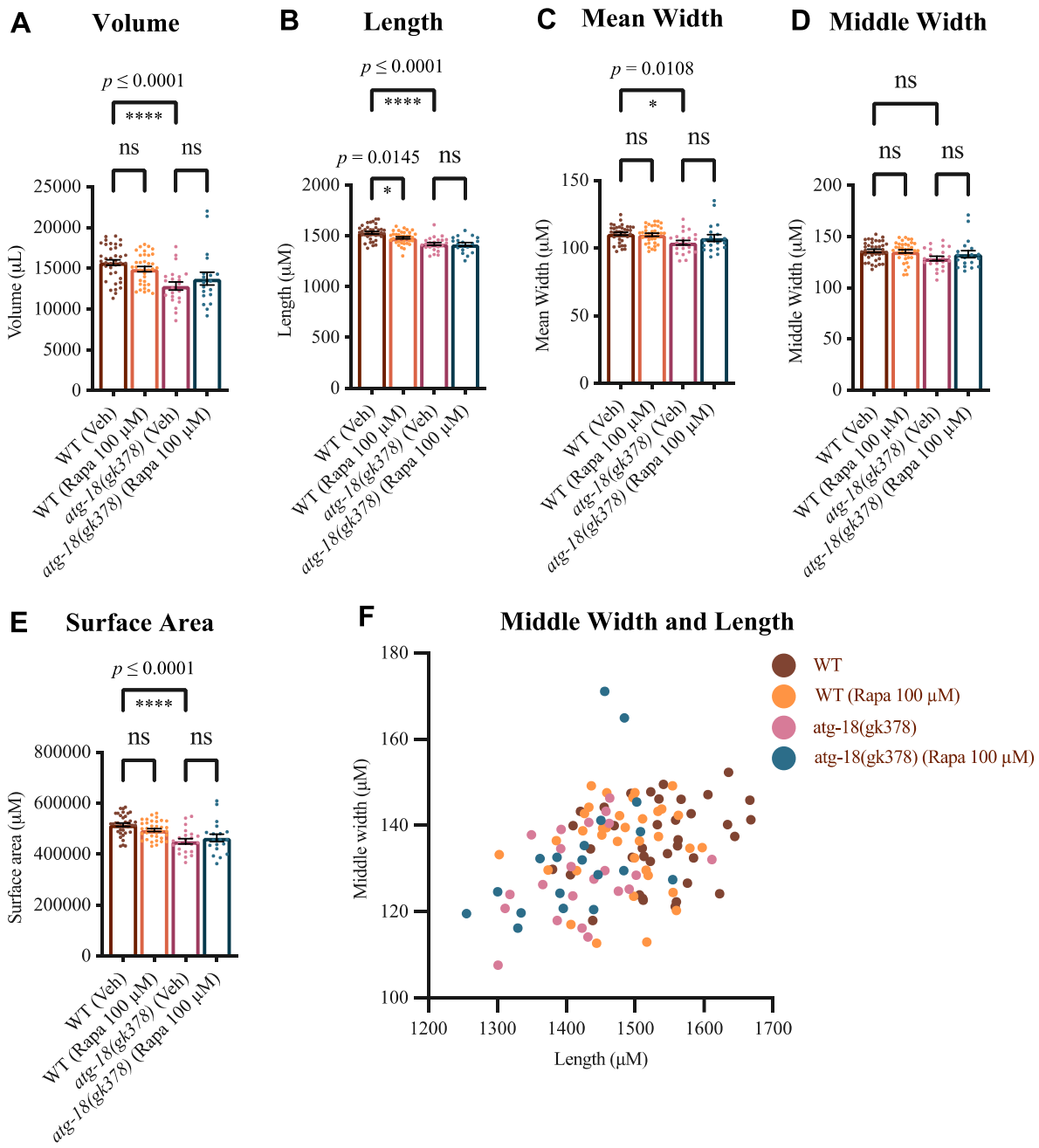

Figure 8. The effects of rapamycin on the body size of C. elegans atg-18(gk378) mutants. *The graphs show the effects of rapamycin on the body size of the mutants and the WTs. In body volume (A), there is only a significant ($p \leq 0.0001$) decrease in the volume of the mutant compared to the WT, both without treatment. In body length (B), the body of the non-treated mutant is significantly ($p \leq 0.0001$) shorter than the non-treated WT, and the body of the rapamycin-treated WT is also significantly ($p = 0.0145$) shorter than the non-treated WT. In mean width (C), there is only a significant ($p = 0.0108$) decrease in the width of the mutant compared to the WT, both without treatment. For middle width (D), no significant differences are shown. The surface area (E) of the non-treated mutants is significantly ($p \leq 0.0001$) smaller than the non-treated WT. (F) shows that the WT worms are generally bigger than the mutants when comparing middle with and length. For the statistical results in (A-E), Ordinary one-way ANOVA with Tukey's multiple comparisons test was used. The error bars are the standard error of the mean.*

4.2 The effects of rapamycin on autophagy in HeLa GFP-WIPI2B cells

4.2.1 The effects of rapamycin on cell intensity and foci formation in HeLa GFP-WIPI2B cells

To investigate the effects of rapamycin on HeLa cells with GFP-tagged WIPI2B, cell cultures were treated with 100 μM rapamycin. Cells treated with DMSO were used as a negative control (Vehicle), while cells treated with EBSS that causes starvation, and hence autophagy were used as positive control. The cells treated with DMSO, EBSS and rapamycin were live-imaged after 2 hours of treatment, and rapamycin-treated cells were also imaged after 24 hours of treatment. This was done to examine the GFP-intensity and foci formation in the cells to investigate whether rapamycin induces WIPI2B-dependent autophagy, and if rapamycin-treatment affect WIPI2B. Because WIPI2B are tagged with GFP, one foci in a cell corresponds to one autophagosome biogenesis event, meaning more foci represents a greater degree of autophagy in the cells.

10-16 images were taken per treatment group (counting rapamycin treatment for 2 hours and 24 hours as different groups), resulting in images of 79-108 cells per group. The images were analyzed with ImageJ where the mean GFP-intensity and number of foci in each cell were found. The results were plotted in GraphPad Prism 9 where all plots and statistical analyzes were made. The statistical analyzes were done using Ordinary one-way ANOVA with Dunnett's multiple comparisons test, **** $p \leq 0.0001$, *** $p \leq 0.001$, ** $p \leq 0.01$, * $p \leq 0.05$ and (ns) $p > 0.05$.

Visually looking at the images of the cells, the cells show a huge variation in intensity, but apparently with no difference depending on the treatment. The statistical analyzes partially confirms this, with no significant difference in mean intensity between the Vehicle and EBSS-treatment, or between the Vehicle and 24-hour rapamycin-treatment (**Fig. 9A**). On the other hand, a significant ($p = 0.0064$) decrease in mean intensity per cell is shown for the cells with 2-hour treatment of rapamycin compared to Vehicle (**Fig. 9A**). For the number of foci formations, the statistical analyzes (**Fig. 9B**) corresponds with what is visually seen in the images (**Fig. 9C-F**). That is, a 24-hour treatment with rapamycin increases the foci formation and hence induces WIPI2B-dependent autophagy. In the positive control with EBSS-treatment, the number of foci is significantly ($p \leq 0.0001$) increased compared to Vehicle. Rapamycin-treatment for 2 hours do not increase the foci formation in the cells, but a 24-hour treatment

increases the foci formation significantly ($p \leq 0.0001$) compared to Vehicle (**Fig. 9B**). **Figure 9C** shows some foci formation in the Veh, indicating some autophagy in the cells. **Figure 9D** show cells treated with EBSS. More foci are shown here, indicating that the starvation increases the autophagy. After 2-hour rapamycin treatment (**Fig. 9E**), some foci are shown, but not as many as for the EBSS-treatment. After 24-hours of rapamycin-treatment, the images (**Fig. 9F**) show a lot of foci formation in the cells, indicating a high increase of autophagy after this treatment.

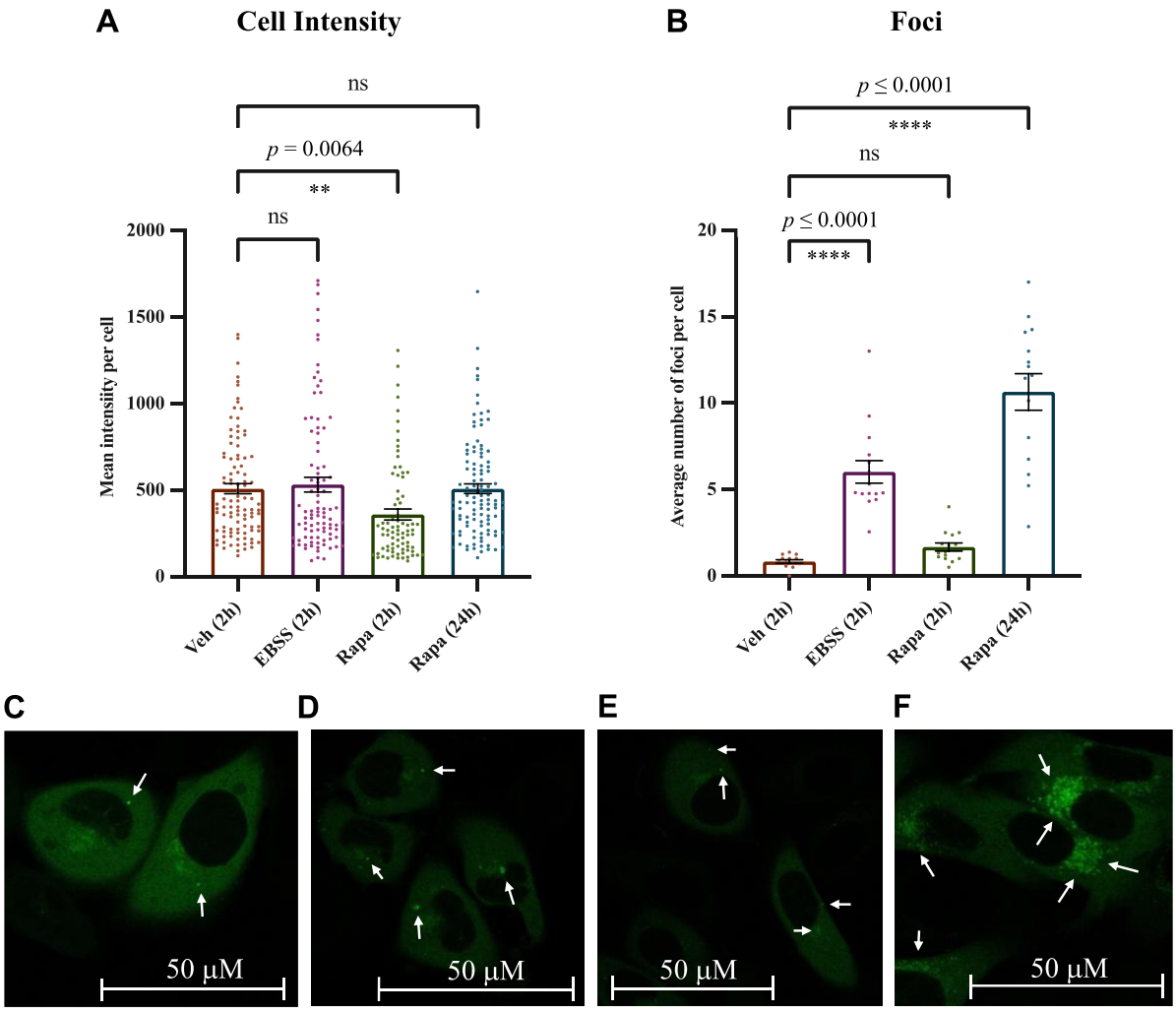

Figure 9. The effects of rapamycin on cell intensity and foci formation in HeLa GFP-WIPI2B. *(A) The cell intensity is significantly (p = 0.0064) decreased in the cells after 2 hours of rapamycin-treatment. EBSS-treatment and 24-hour rapamycin-treatment does not show a significant difference in mean intensity per cell. (B) 2-hour starvation of the cells with EBSS-treatment significantly (p ≤ 0.0001) increase the average number of foci per cell. 2-hour treatment with rapamycin does not show a difference in the number of foci. 24-hours of rapamycin-treatment show a significant (p ≤ 0.0001) increase in the average number of foci per cell. Ordinary one-way ANOVA with Dunnett's multiple comparisons test was used for the statistical results in (A) and (B). The error bars are the standard error of the mean. Foci formation is shown in different rates in 2-hour DMSO treated cells*

(Vehicle, negative control) (C), in EBSS-treated cells (positive control) (D), after 2-hour rapamycin-treatment (E), and after 24-hour rapamycin-treatment (F). White arrows are pointing at some foci in the cells.

4.2.2 Western Blot of autophagy-related proteins

The Western Blot analysis were performed to examine the presence of different autophagy-related proteins in the HeLa cells after the different treatments: DMSO (Vehicle, negative control), EBSS (positive control), and rapamycin. The Western Blot was done in three replicates for each of the treatments. The detected Western Blots were quantified using the ImageJ software, and the resulting fold change compared to Vehicle were plotted in GraphPad Prism 9 where all graphs and statistical analysis were made. Ordinary one-way ANOVA with Dunnett's multiple comparisons test (**** $p \leq 0.0001$, *** $p \leq 0.001$, ** $p \leq 0.01$, * $p \leq 0.05$ and (ns) $p > 0.05$) was used to compare the amount of proteins for each group and to calculate the statistical differences.

Figure 10A and **10B** shows the detected Western Blots of all the autophagy-proteins of interest: mTOR, ULK1, ATG-7, p62, BCL-2, LC3BI, LC3BII, AMBRA1, and Parkin. The fold change compared to Vehicle for all samples is shown in the **Figures 10C-10K**. The amount of the proteins mTOR (**Fig. 10C**), LC3BII (**Fig. 10E**), ATG-7 (**Fig. 10G**) and p62 (**Fig. 10I**) do not differ significantly in any of the different treated cells. 2-hour rapamycin treatment significantly ($p = 0.0320$) increases the amount of LC3BI in the cells compared to Vehicle (**Fig. 10D**). This treatment also increases the amount of BCL-2 (**Fig. 10J**) significantly ($p = 0.0289$) compared to Vehicle. The amount of ULK-1 (**Fig. 10H**) and AMBRA1 (**Fig. 10K**) are significantly decreased (ULK-1: $p = 0.0236$, AMBRA1: $p = 0.0459$) in the cells with EBSS-treatment compared to Vehicle.

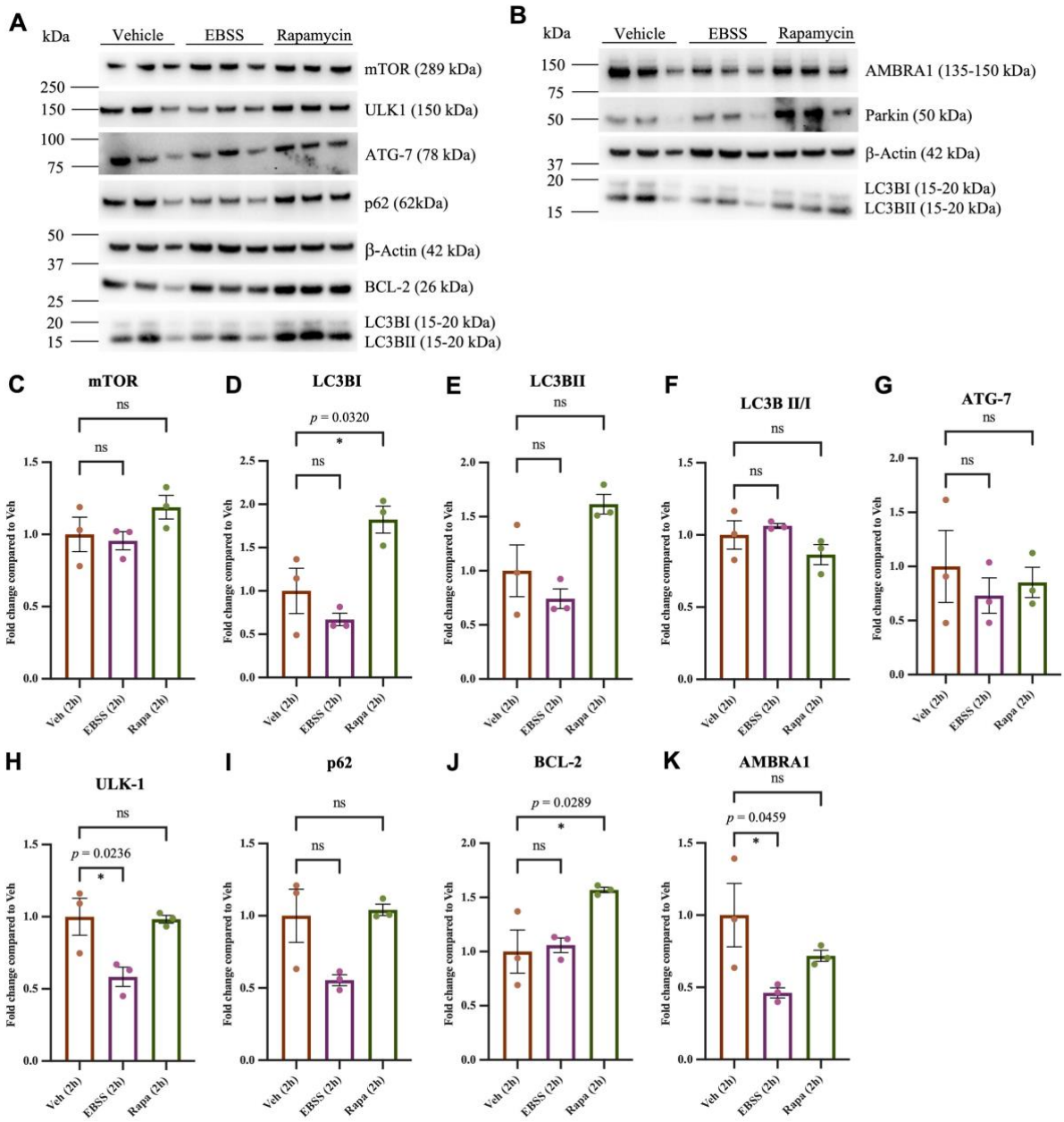

Figure 10. Western Blot analysis of selected autophagy-related proteins in cells treated with rapamycin. *Western Blot analysis of the autophagy-related proteins mTOR, ULK1, ATG-7, p62, BCL-2, LC3BI, and LC3BII (A), and AMBRA1, Parkin, LC3BI and LC3BII (B) in cells treated with DMSO for 2 hours (Vehicle), EBSS for 2 hours and rapamycin for 2 hours, in three replicates. β-Actin are the "household" protein in (A) and (B). (C-K) represent graphs with corresponding statistical analyses of the Western Blot results. The different treatments give no significant difference in the amount of the proteins mTOR (C), LC3BII (E), the ratio LC3B II/I (F), ATG-7 (G), or p62 (I). The amount of LC3BI is significantly (p = 0.0320) higher in cells treated with rapamycin, than in the Vehicle cells (D). The amount of ULK-1 is significantly (p = 0.0236) lower in cells treated with EBSS than in Vehicle cells (H). Cells treated with rapamycin have a significantly (p = 0.0289) higher amount of BCL-2 than Vehicle cells (J), and the cells treated with EBSS have a significantly (p = 0.0459) lower amount of AMBRA1 than the Vehicle cells (K). Ordinary one-way ANOVA with Dunnett's multiple comparisons test was used for the statistical results in (C-K). The error bars are the standard error of the mean.*

5 Discussion

The aim of this study was to investigate the role of rapamycin in the *C. elegans atg-18(gk378)* strain harboring a loss-of-function mutation in the *atg-18* gene coding for ATG-18, which is shown to be essential for a functional autophagy-machinery. The study also examined the effect of rapamycin on autophagy in human cells without a loss-of-function mutation. In this section, the presented results will be discussed in perspective to previous findings within the field.

5.1 Rapamycin affects lifespan and healthspan in *C. elegans atg-18* mutants

5.1.1 Rapamycin decrease lifespan in *C. elegans atg-18(gk378)* mutants

The significantly decreased lifespan of the mutants compared to the WT seen in **Figure 5** is expected. The loss-of-function mutation in the *atg-18* gene will inhibit the expression of the gene hence the production of ATG-18 proteins. As these proteins holds an essential role of recruiting a protein complex as well as delivery of lipids needed further in the autophagy process, the process will not continue without ATG-18. An intact autophagy-machinery has previously been shown to be essential for lifespan extension in *C. elegans* and several studies have shown that a dysfunctional autophagy-machinery will decrease the lifespan (Hansen et al., 2018; Minnerly et al., 2017; Takacs et al., 2019). Therefore, considering that the mutants are not capable of performing autophagy, their lifespan is expected to decrease compared to WT.

A series of previous studies investigating the effects of rapamycin on lifespan conclude that rapamycin increases the lifespan of nematodes (Johnson et al., 2013; Robida-Stubbs et al., 2012), mice (Blagosklonny, 2010; Harrison et al., 2009; Li et al., 2014) and flies (Bjedov et al., 2010; Blagosklonny, 2010; Lu et al., 2021). However, this was unexpectedly not shown in this study. No significant differences in lifespan were shown between *C. elegans* WT (Vehicle), or WT treated with rapamycin from adult day 1 (**Fig. 5**, **Appendix B**). The lifespan assay was performed in three biological repeats starting at day 1 with 75-105 worms per group, per biological repeat. Due to disappearances and desiccation on the edge of the plates, only 35-76 worms per group per biological repeat were declared dead by senescence and included in the analyzes. The observed unexpected results might be due to a too small sample size, and a larger sample size might be necessary to see an effect of rapamycin in the WT-strain. Larger sample sizes could be considered in future studies. Other methods of applying rapamycin as well as

longer exposure time could also be considered. In this study, rapamycin was added to the NGM-agar, as well as to the OP50 seeded on top of the agar. Considering OP50 being the food source of the worms, rapamycin will most likely be consumed with the food intake. In **Figure 6**, it is shown that the pharyngeal pumping rate drops noticeably from day 4 to day 12. The amount of food intake is determined by the pharyngeal pumping, meaning that the decrease in pumping rate also implies that the consumption of food and rapamycin decreases with age. This might give a shorter exposure-time of the treatment than needed to give an effect on lifespan extension. The worms were still grown on NGM-agar containing rapamycin when the pumping rate ceased, but the effect from this method of treatment might not be sufficient. All worms were transferred to the rapamycin-containing plates on day 1 of adulthood, meaning they were not exposed to any treatment before reaching adulthood. Furter studies with treatment from the embryogenesis state could be considered to examine effects of earlier treatment and expanded exposure time.

Interestingly, treatment with rapamycin significantly decreases the lifespan of the mutants in all biological repeats (**Fig. 5**). These results are specifically interesting due to the lack of an intact autophagy-machinery in these mutants. The observed decrease in lifespan indicates that rapamycin might have an opposite effect on lifespan when the autophagy machinery is not intact compared to the previous studies showing that rapamycin extends lifespan *C. elegans* with an intact autophagy-machinery (even though this was not confirmed in this study). This suggests that rapamycin might affect other aging-related mechanisms, causing a decrease in lifespan when autophagy is not functional. There are currently no known studies investigating the effects of rapamycin in autophagy-deficient strains, making these result interesting for further studies on this effect in *C. elegans* as well as other model organisms.

5.1.2 Rapamycin increase healthspan in *C. elegans atg-18(gk378)* mutants

The observed overall decrease in pharyngeal pumping with age in both WT and mutants (**Fig. 6**) is expected, and in line with studies implying a positive correlation between pharyngeal pumping and lifespan (Huang et al., 2004). This can also serve as an explanation for the significantly decreased pumping rate in the mutants compared to the WT on all tested days (**Fig. 6**). The results from the lifespan assay in **Figure 5** showed a decreased lifespan in the mutants, implying a faster aging of the mutants compared to the WT. As the mutants age faster, their pumping rate will also decrease at an earlier age, which is shown in this study. However, it should be mentioned that even though a decrease in pumping rate with age is shown in WT and

some mutants, other mutants like the long-lived *C. elegans eat-2* mutant is not capable of performing pumping at a rapid rate. This mutant strain ages at a slower rate, but still shows a slow pumping rate throughout life (McKay et al., 2004).

The rapamycin treatment of the WT worms seems to have a different effect on pumping rate in young and old worms. The significantly increased pumping rate by rapamycin-treatment observed in young worms (day 4, **Fig. 6A**) evens out on day 8 (**Fig. 6B**), and after 12 days, rapamycin has decreased the pumping rate significantly (**Fig. 6C**). This change implies that rapamycin might have different effects on pumping rates at different ages, seemingly with a positive effect in young worms, and a negative effect in aged worms. Previous studies have shown that a short period with rapamycin treatment early in the life of *Mus musculus* and *Drosophila melanogaster* prolonged lifespan, and that the same treatment later in life did not show any effect of the lifespan (Aiello et al., 2022; Juricic et al., 2022). This difference in the lifespan-effect with rapamycin treatment early and late in life might be comparable to the observed differences in the pumping results of the WT in **Figure 6** implying that rapamycin has greater effects early in life. However, the treatment in this study starts early in life and lasts throughout life, so it might not be completely comparable to studies were the treatment starts in aged models.

Anti-aging treatment with rapamycin in humans should not start until the completion of growth to ensure inhibition of aging directly (Blagosklonny, 2022). Treatment at an early age could affect developmental growth in a negative matter. However, considering the studies implying a greater effect on lifespan with an early start of the treatment, it can be suggested that rapamycin-treatment should start early in life but not earlier than the completion of growth (Blagosklonny, 2022). This suggestion for human treatment can be compared to the pumping results showing a greater effect of rapamycin early in the life of the *C. elegans* WT. The first day of treatment in this study (day 1 of adulthood) could possibly correspond to humans in their early twentieth and suggest that rapamycin-treatment starting at this age could be beneficial for lifespan extension and improve healthspan (pumping rate) without affecting developmental growth. However, even though *C. elegans* is a good model organism for many reasons, it is still extremely different from humans, and it cannot be readily assumed that all research can be transferable between humans and nematodes, or other model organisms.

It could be interesting to measure the pumping rate at several different days other than the ones in this study, starting from day 1 of adulthood. However, due to the high pumping rate at day

4, manually counting of the pumping rates on earlier days would probably not be possible if the rates are even higher in the earliest days. Automatic methods for measuring the pumping rates exist and could eventually be used in this case. In this study, the number of pumps within 30 seconds were counted, regardless of an irregular rhythm of the pumping rate. Another change in the conduct of this assay could be to make multiple measurements and calculate the average value in cases with irregular rhythm, like done in a study by Huang et al. (Huang et al., 2004).

An interesting aspect of the pumping rate results is that rapamycin treatment in the mutants seems to have an opposite effect on pumping rates than in the WT with a significant difference only on the day where a difference in the WT was not shown (**Fig. 6**). On this day, day 8, rapamycin decreases the pumping rate in the mutants. This is in line with the observations in lifespan, where rapamycin was shown to decrease the lifespan of the mutants. A decrease in lifespan can indicate a faster aging of the worms. Considering this as well as the suggested positive correlation between lifespan and pumping, the decrease in pumping can be expected. However, this cannot be concluded in young and aged worms.

The thrashing rate might be considered a more accurate measure for healthspan than the pumping rate considering these results are more consistent and more in line with what would be expected, at least for the WT. Thrashing can also be considered a more accurate measure for healthspan because it does not depend on food intake or eating behavior, like the pumping rate does. Even though an extended lifespan was not shown for rapamycin-treated WT, rapamycin increases the thrashing rate in this strain, indicating that the treatment makes these worms "healthier" (**Fig. 7**). This is in line with observations from previous studies showing that autophagy promotes healthy aging in *C. elegans* and other model organisms (Aman et al., 2021; Leidal et al., 2018). This trend is also seen for the mutants, but the increase is only significant on day 4. Nevertheless, it is interesting that the rapamycin treatment seems to have a positive effect on thrashing rate, even in the mutants lacking an intact autophagy machinery. Compared to the lifespan assay where rapamycin decreased the lifespan of the mutants, the thrashing results in **Figure 7** are surprising. It would be expected that the rapamycin-treated mutants with shorter lifespan would also show a decreased thrashing rate, but that is not the case. This raises a question to whether a maintenance of functional autophagy is essential for healthy aging, as stated by Aman et al. (Aman et al., 2021). The autophagy-deficient mutants clearly show a decline in lifespan, but still rapamycin treatment seems to be able to promote healthy aging even without functional autophagy.

Both the pumping assay and the thrashing assay performed in this study were done manually and thereby suffers major disadvantages. In both assays, only one worm can be measured at a time, meaning the assay is very time consuming considering a lot of worms need to be measured. It is also prone to errors in the counting since the counting is done manually with a counter by looking directly at the worm through a microscope. During the first days of the *C. elegans* lifespan, both the pumping rate and thrashing rates are relatively high, making it even harder to distinguish between the pumps or thrashes. The pumping might even be in such a high rate that the human ability to press fast enough on a manual counter can fail. In such assays consistency is important and the repeats in the assays should be performed by the same person to avoid differences in performance that will occur between individuals. Automatic measurements of the pumping assay exist but is not used in this study. For a more accurate measure of the thrashing rate, the assay could be performed by recording a video of the thrashing followed by watching and counting in a slower motion.

5.1.3 Uncoupling lifespan and healthspan

Comparing the results from lifespan with the two healthspan assays pumping and thrashing, the lifespan and healthspan results do not always seem to correlate. Even with the studies implying that autophagy extends both lifespan and healthspan (Aman et al., 2021; Hansen et al., 2018; Leidal et al., 2018), it can be asked whether lifespan and healthspan really are intrinsically correlated. The previously mentioned study by Bansal et al. on the correlation between lifespan and healthspan suggest that healthspan parameters is of importance in studies on antiaging interventions, and that lifespan cannot be seen as the only parameter of interest. They claim that the assumption that lifespan-increasing treatments also prolong healthspan is supported by studies where some are limited to only testing animals at younger ages. Conclusions of the study was that lifespan and healthspan parameters often shows a correlation, but also that there are indicators that lifespan and healthspan regulators thus far may be different. Aging research should consider both healthspan and lifespan assays, but not necessarily as correlated (Bansal et al., 2015). The prediction that lifespan and healthspan might not always correlate can provide as an explanation of the uncorrelated results seen **Figures 5-7** in this study.

5.1.4 Effects of rapamycin on body size in *C. elegans atg-18(gk378)* mutants

Overall, rapamycin does not seem to have an impact on any measured size parameter of the worms. The only observed consistent difference is between the WTs and the mutants, where the WTs have significantly greater volume, longer length, wider mean width, and bigger surface area than the mutants (**Fig. 8**). Other studies have showed similar results using *C. elegans* strains with other mutations causing reduced or non-functional autophagy machinery. Aladzsity et al. showed that strains with mutational inactivation of the *unc-51* (an autophagy gene) had a reduced body size due to a decreased cell size. This suggests that at least some autophagy genes are required for normal cell growth (Aladzsity et al., 2007). Autophagy is also suggested to be required for maintaining muscle mass in mice (Masiero et al., 2009). On the other hand, several studies show an opposite effect, where they imply that induction of autophagy is correlated with smaller body size. In mice, autophagy induction is shown associated with significant wight loss (Fernández et al., 2017), and studies have found that a prolonged treatment of rapamycin prevents body weight gain at a normal rate in mice (Aiello et al., 2022; Fang et al., 2013). The only significant difference shown for rapamycin-treatment in this study is shown in **Figure 8B**, where the WT worms with treatment are shorter than without treatment, in line with the latter mentioned studies.

5.2 Rapamycin induces autophagy in human cells

Since the HeLa cells used in this study has GFP-tagged WIPI2B proteins, most green, fluorescent signal detected by the fluorescent microscope are WIPI2B proteins in the cell. Hence, the mean intensity per cell is a measure of the amount of WIPI2B proteins present in the cells. Background noise can also contribute at least to some extend to the intensity. Before the recruitment of the WIPI2B proteins in the autophagy process, they are widely spread in the cells. When the recruitment takes place, the WIPI2B proteins will come together, which is seen as intense green dots (foci) using a fluorescent microscope. Increased number of foci is therefore a measure of increased autophagy. When the job of the WIPI2B proteins in the process is done, they will spread out in the cell again.

The results in **Figure 9A** shows no change in intensity in the cells after 2 hours of EBSS-treatment and after 24 hours of rapamycin treatment compared to Vehicle. The EBSS-treatment is used as a positive control since it should cause starvation and hence, initiation of autophagy. A lack of increase in cell intensity after this treatment indicates that the mean intensity might

not be a reliable parameter to measure autophagy. The number of foci per cell is significantly increased by the EBSS-treatment (**Fig. 9B**), indicating that this treatment induces autophagy in the cells as expected. The difference between the negative control (Vehicle) and the positive control (EBSS) in average number of foci per cell suggests that this parameter is a more precise measure of autophagy in the cell than the mean intensity per cell. The results of the cell intensity also shows that the mean intensity per cell varies a lot within the treatment groups for all the different treatments. Some cells show almost no signal, while others show a high signal. The variation should probably have been lower to consider the measure of intensity as a good parameter to describe autophagy.

Interestingly, there is a significant decrease in mean intensity per cell after 2 hours of rapamycin treatment. Despite the assumption that intensity is not the best measure of autophagy, this drop early in the treatment might be explained by the role and localization of WIPI2B during the autophagy process. WIPI2B proteins are recruited by a pool of PI3P early in the process. WIPI2B then recruits the ATG12-ATG5-ATG16L1 complex, and the process continues (Aman et al., 2021; Hansen et al., 2018). After the formation of autophagosomes, WIPI2B have been detected at both the inner and outer autophagosome-membrane (Grimmel et al., 2015). GFP on the WIPI2B proteins in this study might be quenched and therefore not able to emit fluorescent signal inside the autophagosome due to low pH. This might lead to the decreased mean intensity seen in **Figure 9A**. However, this would imply an induction of autophagy after 2 hours of rapamycin-treatment, and it would be expected to observe an increase in the average number of foci at this point as well. As the number of foci seemingly are increased to some degree at the time of decreased intensity (but not significant), it can be thought that this point (2-hour treatment) is the start of the gathering of WIPI2B proteins, and that some autophagosomes have formed with WIPI2B localized inside.

After 24 hours of rapamycin treatment, the mean intensity per cell has increased back to Vehicle-level, and a significant increase in the average number of foci per cell is observed. The image in **Figure 9F** also shows a clear gathering of WIPI2B seen as intense, green foci. The link between the increase in intensity from 2-hour treatment to 24-hour treatment compared to the average number of foci showing a relatively high increase in number of foci is unclear. It could be thought from the 2-hour results that the gathering of WIPI2B increased the number of foci "at the cost" of lower mean intensity, but this do not seem to be the case due to the increase in intensity after 24 hours. Another explanation could be that the foci after 24 hours of treatment are so intense compared to 2 hours of treatment that the mean intensity increases to Vehicle

level. Even with lack of a clear connection between the mean intensity per cell and average number of foci per cell, the results in **Figure 9B** and **9F** strongly suggests that treatment with rapamycin in human cells induces autophagy after 24 hours, and that WIPI2B are recruited to take part in this process.

The Western Blots were performed to investigate whether the amount of selected autophagy-related proteins of interest increases in cells treated with rapamycin. The results in **Figure 10** does not show any clear increase in the amount of the tested autophagy-related proteins. Since all proteins of interest are proteins with essential roles in the autophagy process (**1.4.1**) it was expected to see an increase in the amounts of these proteins after treatment with rapamycin. However, these results can be explained in relation to the results presented in **Figure 9B**. **Figure 9B** showed no significant increase in number of foci after the 2-hour treatment, indicating that the initiation of autophagy did not take place after 2 hours of rapamycin treatment. The increase in autophagy is not observed until after 24 hours of rapamycin treatment, or at least somewhere between 2 and 24 hours of treatment. The Western Blot was only performed on cells treated with rapamycin for 2 hours, not for 24 hours. This might explain the lack of an increased number of autophagy-related proteins. It might be that a Western Blot of the cells harvested after 24 hours of treatment could show the expected effect of increased autophagy. The only two proteins that were increased after 2-hour treatment with rapamycin were LC3BI and BCL-2. Knowing LC3BI forms during the phagophore elongation, and that BCL-2 can act as an inhibitor of BECN1 (belonging to the PIK3C3 complex) during the membrane nucleation (**1.4.1**), no clear reason for the increase of these proteins is found.

Treatment with EBSS causes starvation in the cells, which in turn initiates autophagy. This treatment is used as a positive control. Not even the EBSS-treatment showed the expected results of increased number of autophagy-proteins, but the 2-hour duration of the treatment might be an explanation of this as well. A longer treatment period might have been needed for the increased protein expression of autophagy proteins.

5.3 Conclusions of the study

The main aim of this study was to investigate the effects of rapamycin on lifespan and healthspan in *C. elegans atg-18(gk378)* mutants unable to perform autophagy. Even though the study failed to reproduce an expected increase in lifespan for WT *C. elegans*, interesting results were obtained for the effects in the mutants. Apparently, treatment with rapamycin in *C. elegans atg-18* mutants seems to decrease the lifespan of the worms. This suggests that rapamycin might not only affect the autophagy-machinery, but also other mechanisms related to the process of aging, with a negative effect. The healthspan effects of rapamycin in the mutants are not perfectly clear, with decreased pumping rate only in middle-aged worms, and clearly increased thrashing rate in early adulthood, but seemingly also in aged worms. The thrashing rate seems to be a better measure of healthspan with more replicable and consistent results, and with no dependency on food intake or eating behavior. With this in mind, rapamycin seems to increase the healthspan of the mutants as well as for the WT. This is particularly interesting considering the lack of autophagy in the mutants and strengthens the suggestion that rapamycin might affect other aging-related mechanisms in addition to autophagy. No clear conclusion can be drawn by seeing lifespan and healthspan as positively correlated, considering the observed negative effects on lifespan and positive effects in healthspan. However, by uncoupling lifespan and healthspan in the research, as suggested by Bansal et al. (Bansal et al., 2015), this study suggest a conclusion that rapamycin decreases the lifespan of *C. elegans atg-18(gk378)* mutants, but to some degree promote healthier aging in these worms.

The sub-aim of this study was to examine the effects of rapamycin in human cells able to perform autophagy to observe if treatment with rapamycin induces autophagy in the cells. After a 24-hour rapamycin treatment of HeLa cells with GFP-tagged WIPI2B, the average number of foci in the cell, representing autophagy events, clearly increased. Considering the average number of foci per cell as the most reliable autophagy parameter in this study, it is shown that treatment with rapamycin induce autophagy in the human cells.

The mechanisms seemingly affected by rapamycin in the *C. elegans* mutants may be interesting for further investigation. Not only in *C. elegans*, but also using other model organisms to investigate the replicability of the results in other models.

6 References

Aiello, G., Sabino, C., Pernici, D., Audano, M., Antonica, F., Gianesello, M., Ballabio, C., Quattrone, A., Mitro, N., Romanel, A., Soldano, A., & Tiberi, L. (2022). Transient rapamycin treatment during developmental stage extends lifespan in Mus musculus and Drosophila melanogaster. *EMBO Rep*, *23*(9), e55299. https://doi.org/10.15252/embr.202255299

Aladzsity, I., Tóth, M. L., Sigmond, T., Szabó, E., Bicsák, B., Barna, J., Regos, A., Orosz, L., Kovács, A. L., & Vellai, T. (2007). Autophagy genes unc-51 and bec-1 are required for normal cell size in Caenorhabditis elegans. *Genetics*, *177*(1), 655-660. https://doi.org/10.1534/genetics.107.075762

Alberts, B., Johnson, A., Lewis, J., Raff, M., Roberts, K., & Walter, P. (2002). Caenorhabditis Elegans: Development from the Perspective of the Individual Cell. In *Molecular Biology of the Cell* (4th ed.). Garland Science. https://www.ncbi.nlm.nih.gov/books/NBK26861/

Aman, Y., Schmauck-Medina, T., Hansen, M., Morimoto, R. I., Simon, A. K., Bjedov, I., Palikaras, K., Simonsen, A., Johansen, T., Tavernarakis, N., Rubinsztein, D. C., Partridge, L., Kroemer, G., Labbadia, J., & Fang, E. F. (2021). Autophagy in healthy aging and disease. *Nat Aging*, *1*(8), 634-650. https://doi.org/10.1038/s43587-021-00098-4

Audesse, A. J., Dhakal, S., Hassell, L. A., Gardell, Z., Nemtsova, Y., & Webb, A. E. (2019). FOXO3 directly regulates an autophagy network to functionally regulate proteostasis in adult neural stem cells. *PLoS Genet*, *15*(4), e1008097. https://doi.org/10.1371/journal.pgen.1008097

Avery, L., & You, Y.-J. (2005-2018). *C. elegans* feeding. In *WormBook: The Online Review of C. elegans Biology [Internet]*. Pasadena (CA). https://www.ncbi.nlm.nih.gov/books/NBK116080/

Bakula, D., & Scheibye-Knudsen, M. (2020). MitophAging: Mitophagy in Aging and Disease. *Front Cell Dev Biol*, *8*, 239. https://doi.org/10.3389/fcell.2020.00239

Bansal, A., Zhu, L. J., Yen, K., & Tissenbaum, H. A. (2015). Uncoupling lifespan and healthspan in Caenorhabditis elegans longevity mutants. *Proc Natl Acad Sci U S A*, *112*(3), E277-286. https://doi.org/10.1073/pnas.1412192112

Baugh, L. R. (2013). To Grow or Not to Grow: Nutritional Control of Development During Caenorhabditis elegans L1 Arrest. *Genetics*, *194*(3), 539-555. https://doi.org/10.1534/genetics.113.150847

Berger, Z., Ravikumar, B., Menzies, F. M., Oroz, L. G., Underwood, B. R., Pangalos, M. N., Schmitt, I., Wullner, U., Evert, B. O., O'Kane, C. J., & Rubinsztein, D. C. (2006). Rapamycin alleviates toxicity of different aggregate-prone proteins. *Hum Mol Genet*, *15*(3), 433-442. https://doi.org/10.1093/hmg/ddi458

Bjedov, I., Toivonen, J. M., Kerr, F., Slack, C., Jacobson, J., Foley, A., & Partridge, L. (2010). Mechanisms of life span extension by rapamycin in the fruit fly Drosophila melanogaster. *Cell Metab*, *11*(1), 35-46. https://doi.org/10.1016/j.cmet.2009.11.010

Blagosklonny, M. V. (2010). Rapamycin and quasi-programmed aging: four years later. *Cell Cycle*, *9*(10), 1859-1862. https://doi.org/10.4161/cc.9.10.11872

Blagosklonny, M. V. (2022). Rapamycin treatment early in life reprograms aging: hyperfunction theory and clinical practice. *Aging (Albany NY)*, *14*(20), 8140-8149. https://doi.org/10.18632/aging.204354

Boland, B., Yu, W. H., Corti, O., Mollereau, B., Henriques, A., Bezard, E., Pastores, G. M., Rubinsztein, D. C., Nixon, R. A., Duchen, M. R., Mallucci, G. R., Kroemer, G., Levine, B., Eskelinen, E. L., Mochel, F., Spedding, M., Louis, C., Martin, O. R., & Millan, M. J. (2018). Promoting the clearance of neurotoxic proteins in neurodegenerative disorders of ageing. *Nat Rev Drug Discov*, *17*(9), 660-688. https://doi.org/10.1038/nrd.2018.109

Brenner, S. (1974). THE GENETICS OF CAENORHABDITIS ELEGANS. *Genetics*, *77*(1), 71-94. https://doi.org/10.1093/genetics/77.1.71

Buckingham, S. D., & Sattelle, D. B. (2009). Fast, automated measurement of nematode swimming (thrashing) without morphometry. *BMC Neuroscience*, *10*(1), 84. https://doi.org/10.1186/1471-2202-10-84

Callaway, E. (2013). Deal done over HeLa cell line. *Nature*, *500*(7461), 132-133. https://doi.org/10.1038/500132a

Cao, S. Q., Wang, H. L., Palikaras, K., Tavernarakis, N., & Fang, E. F. (2023). Chemotaxis assay for evaluation of memory-like behavior in wild-type and Alzheimer's-disease-like C. elegans models. *STAR Protoc*, *4*(2), 102250. https://doi.org/10.1016/j.xpro.2023.102250

Chow, D. K., Glenn, C. F., Johnston, J. L., Goldberg, I. G., & Wolkow, C. A. (2006). Sarcopenia in the Caenorhabditis elegans pharynx correlates with muscle contraction rate over lifespan. *Experimental Gerontology*, *41*(3), 252-260. https://doi.org/https://doi.org/10.1016/j.exger.2005.12.004

Chrienova, Z., Nepovimova, E., & Kuca, K. (2021). The role of mTOR in age-related diseases. *Journal of Enzyme Inhibition and Medicinal Chemistry*, *36*, 1679-1693. https://doi.org/10.1080/14756366.2021.1955873

Consortium, C. E. S. (1998). Genome sequence of the nematode C. elegans: a platform for investigating biology. *Science*, *282*(5396), 2012-2018. https://doi.org/10.1126/science.282.5396.2012

Corsi, A. K., Wightman, B., & Chalfie, M. (2015). A Transparent window into biology: A primer on Caenorhabditis elegans. *WormBook*, 1-31. https://doi.org/10.1895/wormbook.1.177.1

Fang, Y., Westbrook, R., Hill, C., Boparai, Ravneet K., Arum, O., Spong, A., Wang, F., Javors, Martin A., Chen, J., Sun, Liou Y., & Bartke, A. (2013). Duration of Rapamycin Treatment Has Differential Effects on Metabolism in Mice. *Cell Metabolism*, *17*(3), 456-462. https://doi.org/https://doi.org/10.1016/j.cmet.2013.02.008

Félix, M.-A., & Braendle, C. (2010). The natural history of Caenorhabditis elegans. *Current Biology*, *20*(22), R965-R969. https://doi.org/https://doi.org/10.1016/j.cub.2010.09.050

Fernández, Á. F., Bárcena, C., Martínez-García, G. G., Tamargo-Gómez, I., Suárez, M. F., Pietrocola, F., Castoldi, F., Esteban, L., Sierra-Filardi, E., Boya, P., López-Otín, C., Kroemer, G., & Mariño, G. (2017). Autophagy couteracts weight gain, lipotoxicity and pancreatic β-cell death upon hypercaloric pro-diabetic regimens. *Cell Death & Disease*, *8*(8), e2970-e2970. https://doi.org/10.1038/cddis.2017.373

Fielenbach, N., & Antebi, A. (2008). C. elegans dauer formation and the molecular basis of plasticity. *Genes Dev*, *22*(16), 2149-2165. https://doi.org/10.1101/gad.1701508

García-Prat, L., Martínez-Vicente, M., Perdiguero, E., Ortet, L., Rodríguez-Ubreva, J., Rebollo, E., Ruiz-Bonilla, V., Gutarra, S., Ballestar, E., Serrano, A. L., Sandri, M., & Muñoz-Cánoves, P. (2016). Autophagy maintains stemness by preventing senescence. *Nature*, *529*(7584), 37-42. https://doi.org/10.1038/nature16187

Glenn, C. F., Chow, D. K., David, L., Cooke, C. A., Gami, M. S., Iser, W. B., Hanselman, K. B., Goldberg, I. G., & Wolkow, C. A. (2004). Behavioral deficits during early stages of aging in Caenorhabditis elegans result from locomotory deficits possibly linked to muscle frailty. *J Gerontol A Biol Sci Med Sci*, *59*(12), 1251-1260. https://doi.org/10.1093/gerona/59.12.1251

Grimmel, M., Backhaus, C., & Proikas-Cezanne, T. (2015). WIPI-Mediated Autophagy and Longevity. *Cells*, *4*(2), 202-217. https://doi.org/10.3390/cells4020202

Hansen, M., Rubinsztein, D. C., & Walker, D. W. (2018). Autophagy as a promoter of longevity: insights from model organisms. *Nat Rev Mol Cell Biol*, *19*(9), 579-593. https://doi.org/10.1038/s41580-018-0033-y

Harrison, D. E., Strong, R., Sharp, Z. D., Nelson, J. F., Astle, C. M., Flurkey, K., Nadon, N. L., Wilkinson, J. E., Frenkel, K., Carter, C. S., Pahor, M., Javors, M. A., Fernandez, E., & Miller, R. A. (2009). Rapamycin fed late in life extends lifespan in genetically heterogeneous mice. *Nature*, *460*(7253), 392-395. https://doi.org/10.1038/nature08221

Hering, I., Le, D. T., & von Mikecz, A. (2022). How to keep up with the analysis of classic and emerging neurotoxins: Age-resolved fitness tests in the animal model Caenorhabditis elegans - a step-by-step protocol. *Excli j*, *21*, 344-353. https://doi.org/10.17179/excli2021-4626

Holtze, S., Gorshkova, E., Braude, S., Cellerino, A., Dammann, P., Hildebrandt, T. B., Hoeflich, A., Hoffmann, S., Koch, P., Terzibasi Tozzini, E., Skulachev, M., Skulachev, V. P., & Sahm, A. (2021). Alternative Animal Models of Aging Research [Review]. *Frontiers in Molecular Biosciences*, *8*. https://doi.org/10.3389/fmolb.2021.660959

Hou, Y., Dan, X., Babbar, M., Wei, Y., Hasselbalch, S. G., Croteau, D. L., & Bohr, V. A. (2019). Ageing as a risk factor for neurodegenerative disease. *Nature Reviews Neurology*, *15*(10), 565-581. https://doi.org/10.1038/s41582-019-0244-7

Hu, W., Chen, S., Thorne, R. F., & Wu, M. (2019). TP53, TP53 Target Genes (DRAM, TIGAR), and Autophagy. *Adv Exp Med Biol*, *1206*, 127-149. https://doi.org/10.1007/978-981-15-0602-4_6

Huang, C., Xiong, C., & Kornfeld, K. (2004). Measurements of age-related changes of physiological processes that predict lifespan of Caenorhabditis elegans. *Proc Natl Acad Sci U S A*, *101*(21), 8084-8089. https://doi.org/10.1073/pnas.0400848101

Ibáñez-Ventoso, C., Herrera, C., Chen, E., Motto, D., & Driscoll, M. (2016). Automated Analysis of C. elegans Swim Behavior Using CeleST Software. *J Vis Exp*(118). https://doi.org/10.3791/54359

Ivanković, M., Ćukušić, A., Gotić, I., Škrobot, N., Matijašić, M., Polančec, D., & Rubelj, I. (2007). Telomerase activity in HeLa cervical carcinoma cell line proliferation. *Biogerontology*, *8*(2), 163-172. https://doi.org/10.1007/s10522-006-9043-9

Iwasa, H., Yu, S., Xue, J., & Driscoll, M. (2010). Novel EGF pathway regulators modulate C. elegans healthspan and lifespan via EGF receptor, PLC-gamma, and IP3R activation. *Aging Cell*, *9*(4), 490-505. https://doi.org/10.1111/j.1474-9726.2010.00575.x

Johnson, S. C., Rabinovitch, P. S., & Kaeberlein, M. (2013). mTOR is a key modulator of ageing and age-related disease. *Nature*, *493*(7432), 338-345. https://doi.org/10.1038/nature11861

Juricic, P., Lu, Y.-X., Leech, T., Drews, L. F., Paulitz, J., Lu, J., Nespital, T., Azami, S., Regan, J. C., Funk, E., Fröhlich, J., Grönke, S., & Partridge, L. (2022). Long-lasting geroprotection from brief rapamycin treatment in early adulthood by persistently increased intestinal autophagy. *Nature Aging*, *2*(9), 824-836. https://doi.org/10.1038/s43587-022-00278-w

Kaletta, T., & Hengartner, M. O. (2006). Finding function in novel targets: C. elegans as a model organism. *Nature Reviews Drug Discovery*, *5*(5), 387-399. https://doi.org/10.1038/nrd2031

Keith, S. A., Amrit, F. R. G., Ratnappan, R., & Ghazi, A. (2014). The C. elegans healthspan and stress-resistance assay toolkit. *Methods*, *68*(3), 476-486. https://doi.org/https://doi.org/10.1016/j.ymeth.2014.04.003

Klass, M. R. (1983). A method for the isolation of longevity mutants in the nematode Caenorhabditis elegans and initial results. *Mech Ageing Dev*, *22*(3-4), 279-286. https://doi.org/10.1016/0047-6374(83)90082-9

Landry, J. J. M., Pyl, P. T., Rausch, T., Zichner, T., Tekkedil, M. M., Stütz, A. M., Jauch, A., Aiyar, R. S., Pau, G., Delhomme, N., Gagneur, J., Korbel, J. O., Huber, W., & Steinmetz, L. M. (2013). The Genomic and Transcriptomic Landscape of a HeLa Cell Line. *G3 Genes|Genomes|Genetics*, *3*(8), 1213-1224. https://doi.org/10.1534/g3.113.005777

Leeman, D. S., Hebestreit, K., Ruetz, T., Webb, A. E., McKay, A., Pollina, E. A., Dulken, B. W., Zhao, X., Yeo, R. W., Ho, T. T., Mahmoudi, S., Devarajan, K., Passegué, E., Rando, T. A., Frydman, J., & Brunet, A. (2018). Lysosome activation clears aggregates and enhances quiescent neural stem cell activation during aging. *Science*, *359*(6381), 1277-1283. https://doi.org/10.1126/science.aag3048

Leidal, A. M., Levine, B., & Debnath, J. (2018). Autophagy and the cell biology of age-related disease. *Nature Cell Biology*, *20*(12), 1338-1348. https://doi.org/10.1038/s41556-018-0235-8

Li, J., Kim, S. G., & Blenis, J. (2014). Rapamycin: one drug, many effects. *Cell Metab*, *19*(3), 373-379. https://doi.org/10.1016/j.cmet.2014.01.001

Lopez-Otin, C., Blasco, M. A., Partridge, L., Serrano, M., & Kroemer, G. (2013). The hallmarks of aging. *Cell*, *153*(6), 1194-1217. https://doi.org/10.1016/j.cell.2013.05.039

Lopez-Otin, C., Blasco, M. A., Partridge, L., Serrano, M., & Kroemer, G. (2023). Hallmarks of aging: An expanding universe. *Cell*, *186*(2), 243-278. https://doi.org/10.1016/j.cell.2022.11.001

Lu, Y. X., Regan, J. C., Eßer, J., Drews, L. F., Weinseis, T., Stinn, J., Hahn, O., Miller, R. A., Grönke, S., & Partridge, L. (2021). A TORC1-histone axis regulates chromatin organisation and non-canonical induction of autophagy to ameliorate ageing. *Elife*, *10*. https://doi.org/10.7554/eLife.62233

Mahmood, T., & Yang, P.-C. (2012). Western blot: Technique, theory, and trouble shooting [Technical Article]. *North American Journal of Medical Sciences*, *4*(9), 429-434. https://doi.org/10.4103/1947-2714.100998

Masiero, E., Agatea, L., Mammucari, C., Blaauw, B., Loro, E., Komatsu, M., Metzger, D., Reggiani, C., Schiaffino, S., & Sandri, M. (2009). Autophagy Is Required to Maintain Muscle Mass. *Cell Metabolism*, *10*(6), 507-515. https://doi.org/https://doi.org/10.1016/j.cmet.2009.10.008

Masters, J. R. (2002). HeLa cells 50 years on: the good, the bad and the ugly. *Nature Reviews Cancer*, *2*(4), 315-319. https://doi.org/10.1038/nrc775

McKay, J. P., Raizen, D. M., Gottschalk, A., Schafer, W. R., & Avery, L. (2004). eat-2 and eat-18 are required for nicotinic neurotransmission in the Caenorhabditis elegans pharynx. *Genetics*, *166*(1), 161-169. https://doi.org/10.1534/genetics.166.1.161

Menzies, F. M., Fleming, A., & Rubinsztein, D. C. (2015). Compromised autophagy and neurodegenerative diseases. *Nat Rev Neurosci*, *16*(6), 345-357. https://doi.org/10.1038/nrn3961

Minnerly, J., Zhang, J., Parker, T., Kaul, T., & Jia, K. (2017). The cell non-autonomous function of ATG-18 is essential for neuroendocrine regulation of Caenorhabditis elegans lifespan. *PLoS Genet*, *13*(5), e1006764. https://doi.org/10.1371/journal.pgen.1006764

Moore, B. T., Jordan, J. M., & Baugh, L. R. (2013). WormSizer: high-throughput analysis of nematode size and shape. *PLoS One*, *8*(2), e57142. https://doi.org/10.1371/journal.pone.0057142

Naranjo-Galindo, F. J., Ai, R., Fang, E. F., Nilsen, H. L., & SenGupta, T. (2022). C. elegans as an Animal Model to Study the Intersection of DNA Repair, Aging and Neurodegeneration [Review]. *Frontiers in Aging*, *3*. https://doi.org/10.3389/fragi.2022.916118

Niccoli, T., & Partridge, L. (2012). Ageing as a risk factor for disease. *Curr Biol*, *22*(17), R741-752. https://doi.org/10.1016/j.cub.2012.07.024

Noda, T., & Ohsumi, Y. (1998). Tor, a phosphatidylinositol kinase homologue, controls autophagy in yeast. *J Biol Chem*, *273*(7), 3963-3966. https://doi.org/10.1074/jbc.273.7.3963

Poganik, J. R., Zhang, B., Baht, G. S., Tyshkovskiy, A., Deik, A., Kerepesi, C., Yim, S. H., Lu, A. T., Haghani, A., Gong, T., Hedman, A. M., Andolf, E., Pershagen, G., Almqvist, C., Clish, C. B., Horvath, S., White, J. P., & Gladyshev, V. N. (2023). Biological age is increased by stress and restored upon recovery. *Cell Metab*, *35*(5), 807-820.e805. https://doi.org/10.1016/j.cmet.2023.03.015

Reggiori, F., & Klionsky, D. J. (2002). Autophagy in the eukaryotic cell. *Eukaryot Cell*, *1*(1), 11-21. https://doi.org/10.1128/EC.01.1.11-21.2002

Restif, C., Ibáñez-Ventoso, C., Vora, M. M., Guo, S., Metaxas, D., & Driscoll, M. (2014). CeleST: computer vision software for quantitative analysis of C. elegans swim behavior reveals novel features of locomotion. *PLoS Comput Biol*, *10*(7), e1003702. https://doi.org/10.1371/journal.pcbi.1003702

Riddle, D. L., Swanson, M. M., & Albert, P. S. (1981). Interacting genes in nematode dauer larva formation. *Nature*, *290*(5808), 668-671. https://doi.org/10.1038/290668a0

Robida-Stubbs, S., Glover-Cutter, K., Lamming, D. W., Mizunuma, M., Narasimhan, S. D., Neumann-Haefelin, E., Sabatini, D. M., & Blackwell, T. K. (2012). TOR signaling and rapamycin influence longevity by regulating SKN-1/Nrf and DAF-16/FoxO. *Cell Metab*, *15*(5), 713-724. https://doi.org/10.1016/j.cmet.2012.04.007

Sabatini, D. M. (2017). Twenty-five years of mTOR: Uncovering the link from nutrients to growth. *Proceedings of the National Academy of Sciences*, *114*(45), 11818-11825. https://doi.org/doi:10.1073/pnas.1716173114

Scherer, W. F., Syverton, J. T., & Gey, G. O. (1953). Studies on the propagation in vitro of poliomyelitis viruses. IV. Viral multiplication in a stable strain of human malignant epithelial cells (strain HeLa) derived from an epidermoid carcinoma of the cervix. *J Exp Med*, *97*(5), 695-710. https://doi.org/10.1084/jem.97.5.695

Schinaman, J. M., Rana, A., Ja, W. W., Clark, R. I., & Walker, D. W. (2019). Rapamycin modulates tissue aging and lifespan independently of the gut microbiota in Drosophila. *Scientific Reports*, *9*(1), 7824. https://doi.org/10.1038/s41598-019-44106-5

Schindelin, J., Arganda-Carreras, I., Frise, E., Kaynig, V., Longair, M., Pietzsch, T., Preibisch, S., Rueden, C., Saalfeld, S., Schmid, B., Tinevez, J. Y., White, D. J., Hartenstein, V., Eliceiri, K., Tomancak, P., & Cardona, A. (2012). Fiji: an open-source platform for biological-image analysis. *Nat Methods*, *9*(7), 676-682. https://doi.org/10.1038/nmeth.2019

Schmauck-Medina, T., Molière, A., Lautrup, S., Zhang, J., Chlopicki, S., Madsen, H. B., Cao, S., Soendenbroe, C., Mansell, E., Vestergaard, M. B., Li, Z., Shiloh, Y., Opresko, P. L., Egly, J.-M., Kirkwood, T., Verdin, E., Bohr, V. A., Cox, L. S., Stevnsner, T., . . . Fang, E. F. (2022). New hallmarks of ageing: a 2022 Copenhagen ageing meeting summary. *Aging (Albany NY)*, *14*, 6829-6839. https://doi.org/10.18632/aging.204248

Stavoe, A. K. H., Gopal, P. P., Gubas, A., Tooze, S. A., & Holzbaur, E. L. F. (2019). Expression of WIPI2B counteracts age-related decline in autophagosome biogenesis in neurons. *Elife*, *8*, e44219. https://doi.org/10.7554/eLife.44219

Takacs, Z., Sporbeck, K., Stoeckle, J., Prado Carvajal, M. J., Grimmel, M., & Proikas-Cezanne, T. (2019). ATG-18 and EPG-6 are Both Required for Autophagy but Differentially Contribute to Lifespan Control in Caenorhabditis elegans. *Cells*, *8*(3). https://doi.org/10.3390/cells8030236

Tatar, M. (2009). Can we develop genetically tractable models to assess healthspan (rather than life span) in animal models? *J Gerontol A Biol Sci Med Sci*, *64*(2), 161-163. https://doi.org/10.1093/gerona/gln067

Thermo Fisher Scientific Inc. *Pierce™ BCA Protein Assay Kit*. Thermo Scientific™. Retrieved April 28, 2023 from https://www.thermofisher.com/order/catalog/product/23225

Wang, H., Zhao, Y., & Zhang, Z. (2019). Age-dependent effects of floxuridine (FUdR) on senescent pathology and mortality in the nematode Caenorhabditis elegans. *Biochem Biophys Res Commun*, *509*(3), 694-699. https://doi.org/10.1016/j.bbrc.2018.12.161

Wang, Y., & Zhang, H. (2019). Regulation of Autophagy by mTOR Signaling Pathway. In Z.-H. Qin (Ed.), *Autophagy: Biology and Diseases: Basic Science* (pp. 67-83). Springer Singapore. https://doi.org/10.1007/978-981-15-0602-4_3

Yang, Z., & Klionsky, D. J. (2009). An overview of the molecular mechanism of autophagy. *Curr Top Microbiol Immunol*, *335*, 1-32. https://doi.org/10.1007/978-3-642-00302-8_1

Yen, K., Narasimhan, S., & Tissenbaum, H. (2011). DAF-16/Forkhead Box O Transcription Factor: Many Paths to a Single Fork(head) in the Road. *Antioxidants & redox signaling*, *14*, 623-634. https://doi.org/10.1089/ars.2010.3490

Zhang, S., Li, F., Zhou, T., Wang, G., & Li, Z. (2020). Caenorhabditis elegans as a Useful Model for Studying Aging Mutations [Review]. *Frontiers in Endocrinology*, *11*. https://doi.org/10.3389/fendo.2020.554994

7 Appendix A – Materials

7.1 Laboratory equipment

Table A.1. Laboratory equipment. *The table shows all the laboratory equipment used in this study along with the suppliers.*

Category	Equipment	Supplier
Appliances	Autoclave/Steam Sterilizer	Getinge
	Grant-Bio PMR-30 Mini Rocker Shaker	Kisker Biotech
	Freezer, -20°C	Liebherr
	HERA safe sterile hood	Thermo Electron Corporation (Thermo Fisher Scientific)
	Incubator, 37°C	Thermo Fisher Scientific
	Microwave	Sharp
	Multitron Standard Shaker	Infors HT
	Refrigerator, 4°C	Whirlpool and Beko
	Roller mixer SRT6D	Stuart®
	TwinGuard Freezer, -80°C	PHCbi
Centrifuges	Heraeus Multifuge 1S-R Centrifuge	Thermo Electron Corporation (Thermo Fisher Scientific)
	Heraeus Fresco 17 Centrifuge	Thermo Scientific
Instruments	ChemiDoc XRS+ Imaging System	Bio-Rad
	Varioskan, version 3.01.15 (ELISA)	Thermo Electron Corporation (Thermo Fisher Scientific)
Gel Equipment	Blotting Roller	Invitrogen™ – Thermo Fisher Scientific
	Blotting Sponges	Invitrogen™ – Thermo Fisher Scientific
	Blotting Tweezer	Invitrogen™ – Thermo Fisher Scientific
	Filter paper	VWR

	NuPAGE™ 4-12% Bis-Tris Midi Gel	Invitrogen™ – Thermo Fisher Scientific
	Polyvinylidene difluoride (PVDF) transfer membrane	Bio-Rad
	PowerPac™ HC High-Current Power Supply	Bio-Rad
	SureLock™ Tandem Midi Blot Module	Invitrogen™ – Thermo Fisher Scientific
	SureLock™ Tandem Midi Gel Tank	Invitrogen™ – Thermo Fisher Scientific
	SureLock™ Tandem Tray	Invitrogen™ – Thermo Fisher Scientific
Miscellaneous Equipment	Automated Pipettes	Eppendorf® and Thermo Scientific
	Cell scraper	Sarstedt
	Counter	Unknown
	Flame burner (refillable)	Schott
	Glass pipettes	Corning®
	HAAKE SWB25 Water Bath (37°C)	Thermo Electron Corporation (Thermo Fisher Scientific)
	Hemocytometer	BRAND GMBH + CO KG
	JB Nova Digital Water Bath with Lid (55°C)	Grant Instruments™
	Laboratory Bunsen burner	Usbeck
	Microscope slide	GmBH & Co KG
	PIPETBOY2 Pipette Controller	Integra Biosciences™
	Pipette Refill Tips	TipOne® Starlab and Thermo Scientific
	Parafilm® (Laboratory Film)	Sigma-Aldrich
	Serological Pipette	Sarstedt
	Scalpel	Swann-Morton
	Small boxes	Thermo Scientific

	Stuart SBH130D Block heater	Stuart
	Timer	VWR
	VACUBOY Vacuum Hand Operator	Integra Biosciences™
	VACUSAFE Aspiration System	Integra Biosciences™
	MS1 Minishaker Vortex	IKA®
	Worm picker	Made with platinum wire and glass pipette
Microscopes	Leica DMIL Microscope	Leica
	Nikon Eclipse Ti2 Microscope	Nikon
	Stemi 508 Microscope	Zeiss
	Zeiss LSM 780 Confocal Microscope	Zeiss
Tubes, plates, and flasks	1.5 mL Micro Tube	Sarstedt
	15 mL Falcon tube	Sarstedt
	50 mL Falcon tube	Sarstedt
	6-well Tissue Culture Plate	Avantor by VWR
	96-well Microplate	Thermo Scientific
	Glass bottles 1 L	VWR
	IBIDI glass bottom dish	Ibidi
	Petri plates, 60 mm	Sarstedt
	Sterile T75 tissue culture flask	Thermo Scientific

7.2 Chemicals

Table A.2. Chemicals. *The table shows all the chemicals used in this study along with the suppliers.*

Chemical	**Supplier**
0.05% Trypsin-EDTA (1X)	Gibco™ - Thermo Fisher Scientific
100% Methanol	Sigma-Aldrich
$CaCl_2$ (1 M)	Sigma-Aldrich
Chlorine	Orkla
Cholesterol in EtOH	Sigma-Aldrich
DDT (1 M)	Sigma-Aldrich
DMSO	Sigma-Aldrich
Dulbecco's Modified Eagle Medium	Gibco™ - Thermo Fisher Scientific
FBS, Qualified (Fetal Bovine Serum)	Gibco™ - Thermo Fisher Scientific
FUDR (15 mM)	Sigma-Aldrich
K_2HPO_4	Sigma-Aldrich
KH_2PO_4	Sigma-Aldrich
Lysogeny broth	Kindly provided by the Fang Lab
$MgSO_4$ (1 M)	Sigma-Aldrich
Na_2HPO_4	Sigma-Aldrich
NaCl	Sigma-Aldrich
NaOH (5 M)	Sigma-Aldrich
Nonfat Dry Milk (#9999)	Cell Signaling Technology®
NuPAGE™ LDS Sample Buffer (4X)	Invitrogen™ – Thermo Fisher Scientific
NuPAGE™ MES SDS Running Buffer (20X)	Invitrogen™ – Thermo Fisher Scientific
NuPAGE™ Transfer Buffer (20X)	Invitrogen™ – Thermo Fisher Scientific
Penicillin/Streptomycin	Sigma-Aldrich
Peptone	Sigma-Aldrich
Phosphate-buffered saline (PBS)	Kindly made by the kitchen in the 4th floor, Akershus University Hospital
Precision Plus Protein™ Kaleidoscope™ Prestained Protein Standards #1610375	Bio-Rad

Halt™ Protease + phosphatase inhibitor cocktail (100X)	Thermo Scientific
Rapamycin (10 mM)	LC Laboratories
Pierce™ RIPA buffer	Thermo Scientific
Streptomycin sulfate	Sigma-Aldrich
Tris Buffered Saline, (10X)	Sigma-Aldrich
Tween 20	Sigma-Aldrich

7.3 Antibodies

7.3.1 Primary antibodies

Table A.3. Primary antibodies. *The table gives information about the primary antibodies used in this study along with the protein target of the antibody, size of the proteins and the ratio of the antibody and the milk-TBST solution.*

Protein target	**Protein size (kDa)**	**Primary antibody**	**Company**	**Catalog no.**	**Ratio antibody:milk-TBST-solution**
Parkin	50	Parkin Antibody	Cell Signaling Technology	#2132S	1:1000
AMBRA1	135-150	Ambra1 Antibody	Cell Signaling Technology	#24907S	1:1000
ULK1 (S555)	150	ULK1 (R600) Antibody	Cell Signaling Technology	#4773S	1:2000
mTOR (7C10)	289	mTOR (7C10) Rabbit mAb	Cell Signaling Technology	#2983	1:1000
LC3B (I+II)	15-20	LB3B Antibody	Cell Signaling Technology	#2775S	1:1000
ATG-7	78	Atg7 Antibody	Cell Signaling Technology	#2631S	1:1000
BCL-2	26	Bcl-2 (50E3) Rabbit mAb	Cell Signaling Technology	#2870S	1:1000

β-Actin	42	Anti-β-Actin antibody, Mouse monoclonal	Sigma-Aldrich	#A1978	1:10000
p62/ SQSTM1	62	SQSTM1/p62 (D5E2) Rabbit mAb	Cell Signaling Technology	#8025S	1:1000

7.3.2 Secondary antibodies

Table A.4. Secondary antibodies. *The table gives information about the secondary antibodies used in this study along with the protein target of the primary antibody serving as targets for the secondary antibody and the ratio of the antibody and the milk-TBST solution.*

Protein target(s) of the corresponding primary antibody	**Secondary antibody**	**Company**	**Catalog no.**	**Ratio antibody:milk-TBST-solution**
β-Actin	Anti-mouse IgG, HRP-Linked antibody	Cell Signaling Technology	#7076	1:3000
mTOR, LC3B (I+II), AMBRA1, ATG-7, ULK-1, p62/SQSTM1, BCL-2	Anti-rabbit IgG, HRP-Linked antibody	Cell Signaling Technology	#7074	1:3000

7.4 Software

Table A.5. Software. *The table gives information about the software used in this study along with the suppliers and URL.*

Software	**Version**	**Supplier**	**URL**
ImageJ	1.53t	Wayne Rasband and contributors. National Institutes of Health, USA	http://imagej.nih.gov/ij
Microsoft Excel	16.66.1 (22101101)	Microsoft	https://www.microsoft.com/nb-no/microsoft-365/excel
Image Lab™	6.0.0 build 25	Bio-Rad Laboratories	https://www.bio-rad.com/en-no/product/image-lab-software?ID=KRE6P5E8Z
GraphPad Prism 9	9.5.1 (528)	GraphPad Software, LCC	https://www.graphpad.com/
WormSizer (plugin for ImageJ/Fiji)	1.2.5	(Moore et al., 2013)	https://github.com/bradtmoore/wormsizer

8 Appendix B – Statistical results of the lifespan assays

Table B.1. Statistics of 1st biological repeat of the lifespan assay. *The table shows median lifespan in days, mean lifespan ± standard error of the mean, p-values and % of change between the compared groups.*

Experiments	**Groups**	**Median lifespan (day)**	**Mean ± S.E.M. (day)**	**Statistics (*p* values and % change)**
Lifespan 1st biological repeat	WT (n = 74)	15,00	15,91 ± 0,3616	
	WT Rapamycin (n = 71)	16,00	16,49 ± 0,5234	$p = 0.1475^{ns}$ vs. WT (+3.6%)
	atg-18(gk378) (n = 56)	12,00	10,77 ± 0,3371	$p \leq 0.0001^{****}$ vs. WT (-32.3%)
	atg-18(gk378) Rapamycin (n = 42)	10,00	8,095 ± 0,6356	$p \leq 0.0002^{***}$ vs. *atg-18(gk378)* (-24.8%)

Table B.2. Statistics of 2nd biological repeat of the lifespan assay. *The table shows median lifespan in days, mean lifespan ± standard error of the mean, p-values and % of change between the compared groups.*

Experiments	**Groups**	**Median lifespan (day)**	**Mean ± S.E.M. (day)**	**Statistics (p values and % change)**
Lifespan 2nd biological repeat	WT (n = 66)	19,00	18,41 ± 0,3554	
	WT Rapamycin (n = 55)	17,00	17,64 ± 0,4131	$p = 0.5175^{ns}$ vs. WT (-4.2%)
	atg-18(gk378) (n = 49)	13,00	13,06 ± 0,4270	$p \leq 0.0001^{****}$ vs. WT (-29.1%)
	atg-18(gk378) Rapamycin (n = 35)	11,00	12,03 ± 0,3790	$p = 0.0445^{*}$ vs. *atg-18(gk378)* (-7.9%)

Table B.3. Statistics of 3rd biological repeat of the lifespan assay. *The table shows median lifespan in days, mean lifespan ± standard error of the mean, p-values and % of change between the compared groups.*

Experiments	**Groups**	**Median lifespan (day)**	**Mean ± S.E.M. (day)**	**Statistics (p values and % change)**
Lifespan 3rd biological repeat	WT (n = 76)	22,00	21,51 ± 0,6139	
	WT Rapamycin (n = 56)	22,00	21,34 ± 0,5503	p = 0,4430^{ns} vs. WT (-0.8%)
	atg-18(gk378) (n = 72)	16,00	15,35 ± 0,3675	$p \leq 0.0001^{****}$ vs. WT (-28.6%)
	atg-18(gk378) Rapamycin (n = 54)	15,50	14,20 ± 0,3619	p = 0,0006*** vs. *atg-18(gk378)* (-7.5%)

9 Appendix C – Raw data from *C. elegans* experiments

Appendix C includes a lot of raw data and can be found and downloaded from this link:

https://www.dropbox.com/s/iliakrfnuxsbqr9/Appendix%20C%20and%20D.pdf?dl=0

10 Appendix D – Raw data from cell experiments

Appendix D includes a lot of raw data and can be found and downloaded from this link:

https://www.dropbox.com/s/iliakrfnuxsbqr9/Appendix%20C%20and%20D.pdf?dl=0

Norges miljø- og biovitenskapelige universitet
Noregs miljø- og biovitskapelege universitet
Norwegian University of Life Sciences

Postboks 5003
NO-1432 Ås
Norway